

# 7

## Enzyme kinetics, structure, function, and catalysis

One important function performed by proteins is the ability to catalyse chemical reactions. Catalytic function was amongst the first biological roles recognized in proteins through the work of Eduard Buchner and Emil Fischer. They identified and characterized the ability of some proteins to convert reactants into products. These proteins, analogous to chemical catalysts, increased rates of reaction but did not shift the equilibrium formed between products and reactants. The biological catalysts were named enzymes – the name derived from the Greek for ‘in yeast’ – ‘en’ ‘zyme’.

Within all cells every reaction is regulated by the activity of enzymes. Enzymes catalyse metabolic reactions and in their absence reactions proceed at kinetically insignificant rates incompatible with living, dynamic, systems. The presence of enzymes results in reactions whose rates may be enhanced (catalysed) by factors of  $10^{15}$  although enhancements in the range  $10^3$ – $10^9$  are more typical. Enzymes participate in the catalysis of many cellular processes ranging from carbohydrate, amino acid and lipid synthesis, their breakdown or catabolic reactions (see Figure 7.1), DNA repair and replication, transmission of stimuli through neurones, programmed cell death or apoptosis, the blood clotting cascade reactions, the degradation of proteins, and the export and import of proteins across membranes. The list is extensive and for each reaction

the cell employs a unique enzyme tailored via millions of years of evolution to catalyse the reaction with unequalled specificity.

This chapter explores how enzyme structure allows reactions to be catalysed with high specificity and rapidity. In order to appreciate enzyme-catalysed reactions the initial sections deal with simple chemical kinetics introducing the terms applicable to the study of reaction rates. Analysis of chemical kinetics proved to be very important in unravelling mechanisms of enzyme catalysis. Kinetic studies uncovered the properties of enzymes, products and reactants, as well as the steps leading to their formation. *In vivo* enzyme activity differs from that observed *in vitro* by its modulation by other proteins or ligands. The modulation of enzyme activity occurs by several mechanisms but is vital to normal cell function and homeostasis. In principle, regulation allows cells to respond rapidly to environmental conditions, turning on or off enzyme activity to achieve metabolic control under fluctuating conditions. When conditions change and the enzyme is no longer required activity is reduced without wasting valuable cell resources. Feedback mechanisms control enzyme activity and are a feature of allostery. Allosteric enzymes exist within the biosynthetic pathways of all cells.

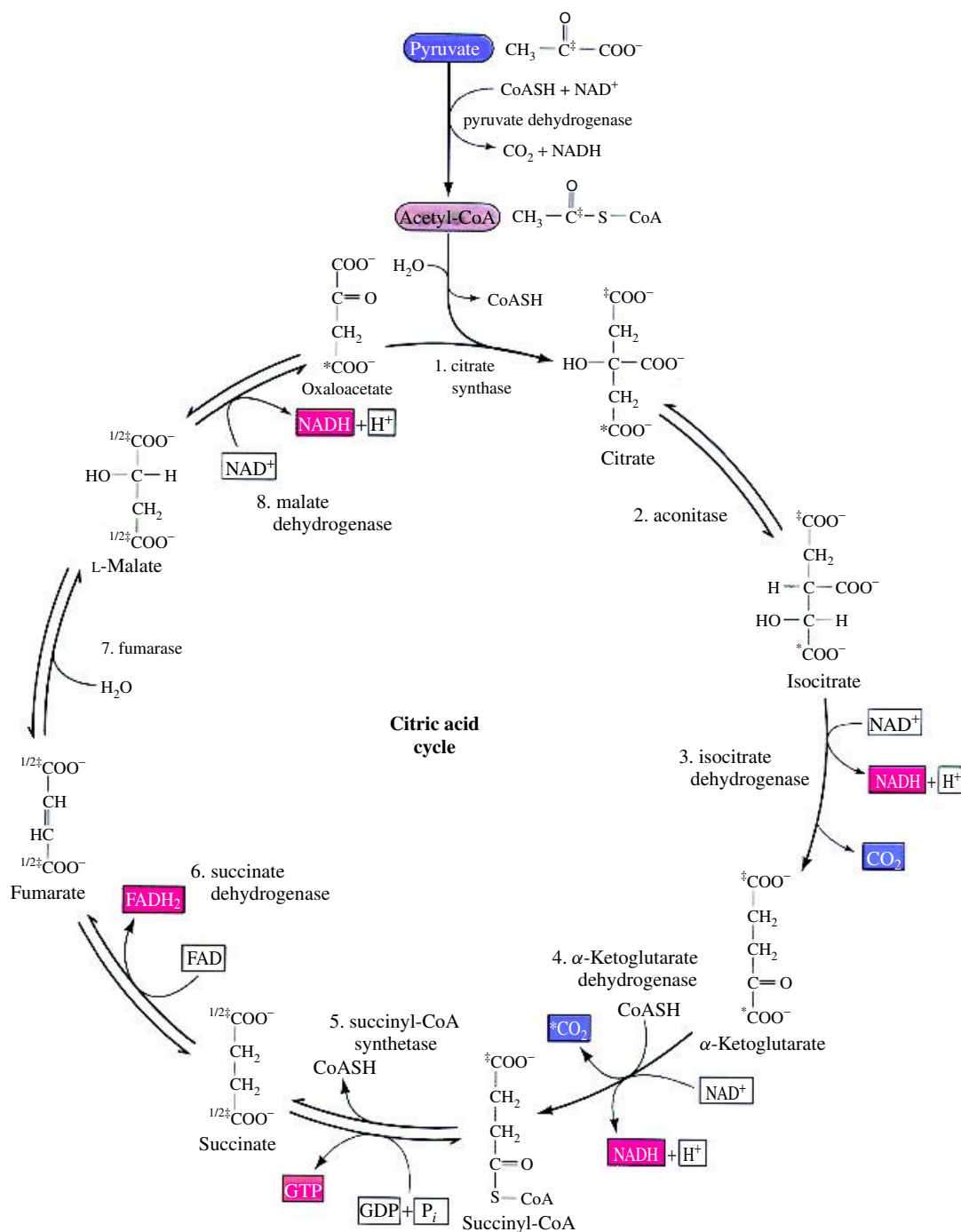
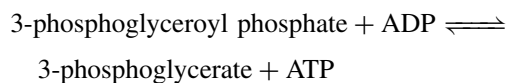


**Figure 7.1** The conversion of pyruvate to acetate from the reactions of glycolysis lead to the Krebs citric acid cycle. Reproduced from Voet *et al.* (1999) by permission of John Wiley & Sons, Ltd. Chichester

**Table 7.1** Examples of enzymes belonging to the six major classes

Enzyme class	Typical example	Reaction catalysed
Oxidoreductases	Lactate dehydrogenase (EC1.1.1.27)	Reduction of pyruvate to lactate with the corresponding formation of NAD
Transferases	Hexokinase (EC 2.7.1.1)	Transfer of phosphate group to glucose from ATP
Hydrolases	Acetylcholinesterase (EC 3.1.1.7)	Hydrolysis of acetylcholine to choline and acetate
Lyases	Phenylalanine Ammonia Lyase (EC 4.3.1.5)	Splits phenylalanine into ammonia and <i>trans</i> -cinnamate
Isomerases	Triose phosphate isomerase (EC 5.3.1.1)	Reversible conversion between dihydroxyacetone phosphate and glyceraldehyde-3-phosphate
Ligases	T4 DNA ligase (EC 6.5.1.1)	Phosphodiester bond linkage and conversion of ATP → AMP

Before reviewing these areas it is necessary to establish the basis of enzyme nomenclature and to establish the broad groups of enzyme-catalysed reactions occurring within all cells. For each catalysed reaction a unique enzyme exists; in glycolysis the conversion of 3-phosphoglycerate phosphate to 3-phosphoglycerate is catalysed by phosphoglycerokinase (PGK).



No other enzyme catalyses this reaction within cells.

## Enzyme nomenclature

The naming of enzymes gives rise to much confusion. Some enzymes have 'trivial' names such as trypsin where the name provides no useful clue to biological role. Many enzymes are named after their coding genes and by convention the gene is written in *italic* script whilst the protein is written in normal type. Examples are the *Escherichia coli* gene *polA* and its product DNA polymerase I; the *lacZ* gene and  $\beta$ -galactosidase. To systematically 'label' enzymes and to help with identification of new enzymes the

International Union of Biochemistry and Molecular Biology (IUBMB) devised a system of nomenclature that divides enzymes into six broad classes (Table 7.1 gives examples of these). Further division into sub-classes groups enzymes sharing functional properties. The major classes of enzyme are:

1. Oxidoreductases: catalyse oxidation–reduction (redox) reactions.
2. Transferases: catalyse transfer of functional groups from one molecule to another.
3. Hydrolases: perform hydrolytic cleavage of bonds.
4. Lyases: remove groups from (or add a group to) a double bond or catalyse bond scission involving electron re-arrangement.
5. Isomerases: catalyse intramolecular rearrangement of atoms.
6. Ligases: joins (ligates) two molecules together.

Each enzyme is given a four-digit number written, for example, as EC 5.3.1.1. The first number indicates an isomerase whilst the second and third numbers identify further sub-classes. In this case the second digit

(3) indicates an isomerase that acts as an intramolecular isomerase whilst the third digit (1) indicates that the substrates for this enzyme are aldose or ketose carbohydrates. The fourth number is a serial number that frequently indicates the order in which the enzyme was recognized. The enzyme EC 5.3.1.1 is triose phosphate isomerase found in the glycolytic pathway catalysing inter-conversion of glyceraldehyde 3 phosphate and dihydroxyacetone phosphate. A complete list of enzyme classes is given in the Appendix. At the end of 2003 the structures of over 8000 enzymes were deposited in the PDB database whilst other databases recognized over 3700 different enzymes (<http://www.expasy.ch/enzyme/>). These lists are continuing to be updated and grow with the completion of further genome sequencing projects.

Until recently it was thought that all biological catalysts (enzymes) were proteins. This view has been revised with the observation that RNA molecules (ribozymes) catalyse RNA processing and protein synthesis. The observation of catalytic RNA raises an interesting and perplexing scenario where RNA synthesis is catalysed by proteins (e.g. RNA polymerase) but protein synthesis is catalysed by RNA (the ribosome). This chapter will focus on the properties and mechanisms of protein based enzymes, in other words those molecules synonymous with the term enzyme.

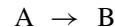
## Enzyme co-factors

Many enzymes require additional co-factors to catalyse reactions effectively. These co-factors, also called co-enzymes, are small organic molecules or metal ions (Figure 7.2). The nature of the interaction between co-factor and enzyme is variable, with both covalent and non-covalent binding observed in biological systems.

A general scheme of classifying co-factors recognizes the strength of their interaction with enzymes. For example, some metal ions are tightly bound at active sites and participate directly in the reaction mechanism whilst others bind weakly to the protein surface and have remote roles (Table 7.2). Co-factors are vital to effective enzyme function and many were recognized originally as vitamins. Alongside vitamins metal ions modulate enzyme activity; in the apo (metal-free) state metalloenzymes often exhibit impaired catalytic activity or decreased stability. The metal ions, normally divalent cations, exhibit a wide range of biological roles (Table 7.3). In carboxypeptidase  $Zn^{2+}$  stabilizes intermediates formed during hydrolysis of peptide bonds whilst in heme and non-heme enzymes iron participates in redox reactions.

## Chemical kinetics

In order to understand the details of enzyme action it is worth reviewing the basics of chemical kinetics since these concepts underpin biological catalysis. For a simple unimolecular reaction where A is converted irreversibly into B



the rate of reaction is given by the rate of disappearance of reactant or the rate of appearance of product

$$-d[A]/dt \text{ or } d[B]/dt \quad (7.1)$$

The disappearance of reactants is proportional to the concentration of A

$$-d[A]/dt = k[A] \quad (7.2)$$

where  $k$  is a first order rate constant (units  $s^{-1}$ ). Rearranging this equation and integrating between

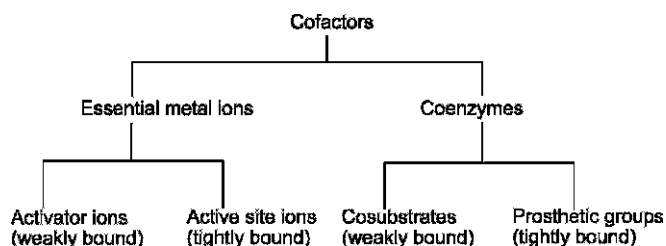


**Figure 7.2** Different co-factors and their interactions with proteins

**Table 7.2** Co-factors found in enzymes together with their biological roles

Component	Co-factor	Metabolic role
Vitamin A	Retinal	Visual cycle.
Thiamine (B <sub>1</sub> )	Thiamine pyrophosphate	Carbohydrate metabolism, transient shuttle of aldehyde groups
Riboflavin (B <sub>2</sub> )	Flavin adenine dinucleotide (FAD) Flavin mononucleotide (FMN).	Redox reactions in flavoenzymes
Niacin (Nicotinic acid)	Nicotinamide adenine dinucleotide (NAD)	Redox reactions involving NAD linked dehydrogenases
Panthenic acid (B <sub>3</sub> )	Coenzyme A	Acyl group activation and transfer
Pyridoxal phosphate (B <sub>6</sub> )	Pyridoxine	Transaminase function
Vitamin B <sub>12</sub>	Cyanocobalamin	Methyl group transfer or intramolecular rearrangement
Folic acid	Tetrahydrofolate	Transfer of formyl or hydroxymethyl groups
Biotin	Biotin	ATP dependent carboxylation of substrates
Vitamin K	Phylloquinone	Carboxylation of Glu residues.
Coenzyme Q	Ubiquinone	Electron and proton transfer

**Table 7.3** Role of metal ions as co-factors in enzyme catalysis

Metal	Metalloenzyme	General reaction catalysed
Fe	Cytochrome oxidase	Reduction of O <sub>2</sub> to H <sub>2</sub> O
Co	Vitamin B <sub>12</sub>	Transfer of methyl groups
Mo	Sulfite oxidase	Reduction of sulfite to sulfate.
Mn	Water splitting enzyme	Photosynthetic splitting of water to oxygen
Ni	Urease	Hydrolysis of urea to ammonia and carbamate
Cu	Superoxide dismutase	Dismutation of superoxide into O <sub>2</sub> and H <sub>2</sub> O <sub>2</sub>
Zn	Carboxypeptidase A	Hydrolysis of peptide bonds

$t = 0$  and  $t = t$  leads to the familiar first order equation

$$-\frac{d[A]}{[A]} = k dt \quad (7.3)$$

$$\int_{[A]_0}^{[A]} \frac{d[A]}{[A]} = - \int_0^t k dt \quad (7.4)$$

$$[A] = [A]_0 e^{-kt} \quad (7.5)$$

A plot of  $\ln([A]/[A]_0)$  versus time ( $t$ ) gives a straight line of slope  $-k$  and provides a graphical method of estimating first order rate constants (Figure 7.3).

An important quantity for any first order reaction is the half-life of the reaction; the time taken for

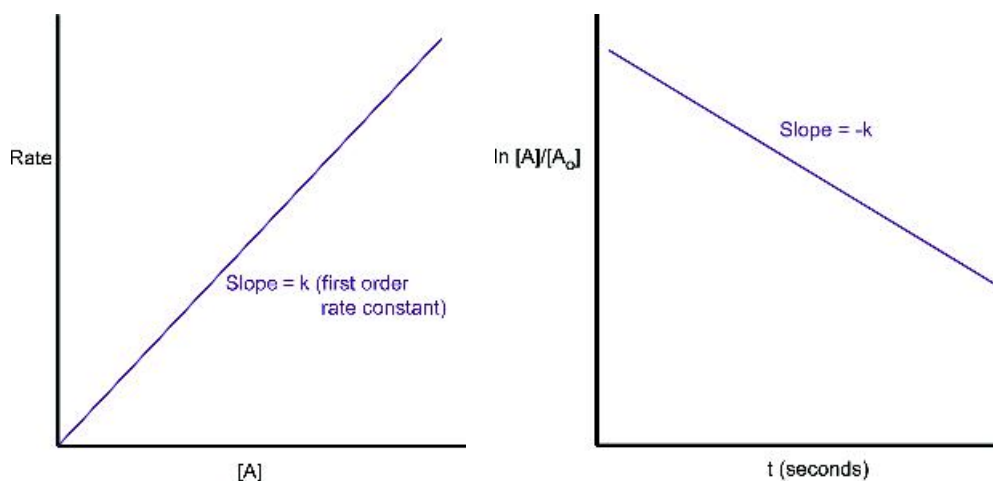


**Figure 7.3** The rate of reaction as function of the concentration of A in the first order reaction of  $A \rightarrow B$  and a graphical plot of  $\ln ([A]/[A]_0)$  versus time ( $t$ ) for the reaction that allows the first order rate constant ( $k$ ) to be estimated

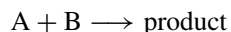
the concentration of the reactant to drop to half its initial value. Rearranging Equation 7.5 yields upon substitution of  $[A] = [A]_0/2$

$$\ln[A]_0/2/[A]_0 = -kt_{1/2} \quad (7.6)$$

where

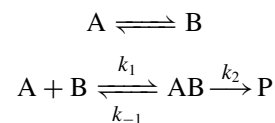
$$t_{1/2} = \ln 2/k = 0.693/k \quad (7.7)$$

Measuring the time for a reactant to fall to half its original concentration allows an estimation of the first order rate constant. In general for a reaction of the  $n$ th order the half life is proportional to  $1/[A]_0^{n-1}$ . These equations occur commonly in reaction kinetics involving biomolecules and extend to related areas such as folding, stability and complex formation. A simple bimolecular reaction is described as an irreversible process where



In contrast the reaction between enzyme and substrate is usually considered as an equilibrium involving forward and backward reactions and it is useful to examine kinetics applicable to (i) a reversible first order reaction and (ii) consecutive reactions,

since these occur frequently in biological studies. Examples include



If we consider the reaction scheme for a reversible reaction defined by forward and backward rate constants of  $k_1$  and  $k_{-1}$  the change in the concentration of A with time is described by the equation

$$-d[A]/dt = k_1[A] - k_{-1}[B] \quad (7.8)$$

with the reverse reaction written similarly as

$$-d[B]/dt = k_{-1}[B] - k_1[A] \quad (7.9)$$

This yields

$$[B]/[A] = k_1/k_{-1} = K_{eq} \quad (7.10)$$

where  $K_{eq}$  is the equilibrium constant for the reaction. A variation occurs when a reversible reaction for conversion of A into B is followed by a consecutive reaction converting B into C. The formation of AB is

a bimolecular reaction between A and B whilst the breakdown of AB to yield P is unimolecular. The easiest way to deal algebraically with this reaction is to describe the formation of AB. This leads to the equation

$$d[AB]/dt = k_1[A][B] - k_{-1}[AB] - k_2[AB] \quad (7.11)$$

Under conditions where either  $k_2 \gg k_1$  or  $k_{-1} \gg k_1$  the concentration of the encounter complex [AB] remains low at all times. This assumption leads to the equality  $d[AB]/dt \approx 0$  and is known as the steady state approximation where

$$k_1[A][B] = k_{-1}[AB] + k_2[AB] \quad (7.12)$$

$$= (k_{-1} + k_2)[AB] \quad (7.13)$$

$$[AB] = k_1[A][B]/(k_{-1} + k_2) \quad (7.14)$$

The rate of formation of product P is described by the rate of breakdown of AB

$$d[P]/dt = k_2[AB] \quad (7.15)$$

$$= k_2 k_1 [A][B]/(k_{-1} + k_2) \quad (7.16)$$

By assimilating the terms  $k_2 k_1/(k_{-1} + k_2)$  into a constant called  $k_{\text{obs}}$  the bimolecular reaction  $A + B \rightarrow AB \rightarrow P$  can be described as a one step reaction governed by a single rate constant ( $k_{\text{obs}}$ ).

In the above equation two interesting boundary conditions apply. When the dissociation of AB reflected by the constant  $k_{-1}$  is much smaller than the rate  $k_2$  ( $k_{-1} \ll k_2$ ) then the overall reaction  $k_{\text{obs}}$  approximates to  $k_1$  and is the diffusion-controlled rate. The second condition applies when  $k_2 \ll k_{-1}$  and is known as the reaction-controlled rate leading to an observed rate constant of

$$k_{\text{obs}} = k_2 k_1 / k_{-1} \quad (7.17)$$

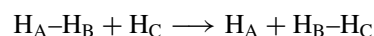
or

$$k_{\text{obs}} = K_{\text{eq}} k_2 \quad (7.18)$$

## The transition state and the action of enzymes

Understanding enzyme action was assisted by transition state theory developed by Henry Eyring from the 1930s

onwards. For a bimolecular reaction involving three atoms there exists an intermediate state of high energy that reflects the breaking of one covalent bond and the formation of a new one. For the reaction of a hydrogen atom with a molecule of hydrogen this state equates to the breakage of the  $H_A-H_B$  bond and the formation of a new  $H_B-H_C$  bond.



An intermediate called the transition state is denoted by the symbol “‡”. The free energy associated with the transition state,  $\Delta G^\ddagger$ , is higher than the free energy associated with either reactant or products (Figure 7.4).

Eyring formulated the transition state in quantitative terms where reactants undergo chemical reactions by their respective close approach along a path of minimum free energy called the reaction coordinate. Reactions are expressed by transition state diagrams that reflect changes in free energy as a function of reaction coordinate. Favourable reactions have negative values for  $\Delta G$  ( $\Delta G < 0$ ) and are called exergonic. Other reactions require energy to proceed and are described as endergonic ( $\Delta G > 0$ ). The free energy changes as the reaction progresses from reactants to product. For the reaction  $R \rightarrow P$  we identify average free energies associated with R and P, as  $G_R$  and  $G_P$ , respectively, with the free energy associated with the products being lower than that of the reactants; the change in free energy is negative and the reaction is favourable. However, although the reaction is favourable the profile does not reveal anything about the rate of reaction nor does it offer any clues about why some reactions occur faster than others.

The concept of activation energy recognized by Arrhenius in 1889 from the temperature dependence of reactions follows the relationship

$$k = A \exp^{-E_a/RT} \quad (7.19)$$

where  $k$  is a rate constant,  $A$  is a frequency factor and  $E_a$  is the activation energy. Eyring realized that a new view of chemical reactions could be obtained by postulating an intermediate, the transition state, occurring between products and reactants. The

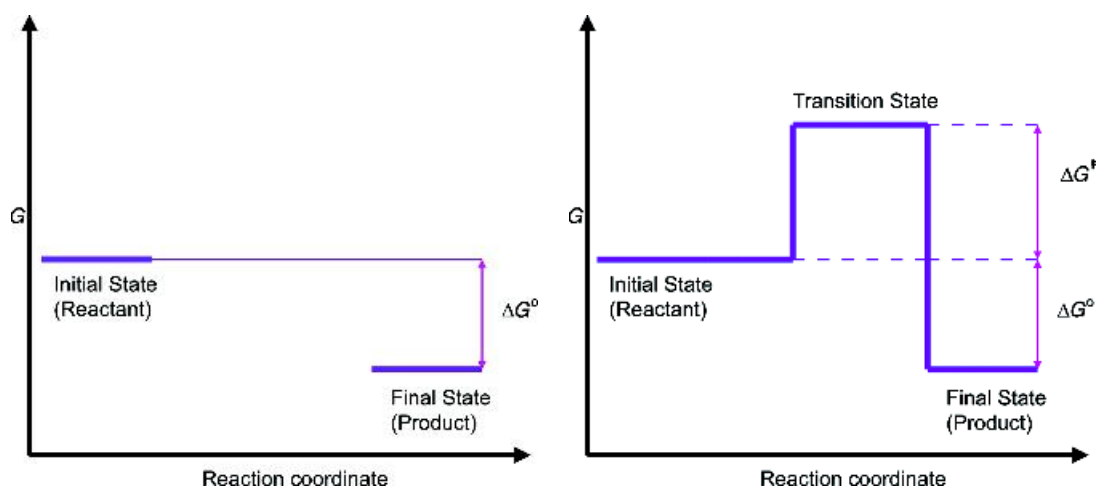
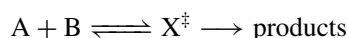


**Figure 7.4** Transition state diagrams. In the absence of a transition state the pathway from reactants to products is obscure but one can recognize that the products have a lower free energy than the reactants ( $G_P < G_R$ )

transition state exists for approximately  $10^{-13}$ – $10^{-14}$  s leading to a small percentage of reactants being found in this conformation at any one time. The formation of product required crossing the activation barrier otherwise the transition state decomposed back to the reactants. With this view of a chemical reaction the rate-limiting step became the decomposition of the transition state to products or reactants involving a non-conventional equilibrium established between reactants and the transition state. For the reaction



the equilibrium constant ( $K^\ddagger$ ) is expressed in terms of the activated complex ( $X^\ddagger$ ) and the reactants (A and B).

$$K^\ddagger = X^\ddagger/[A][B] \quad (7.20)$$

The rate of the reaction is simply the product of the concentration of activated complex multiplied by the frequency of crossing the activation barrier ( $\nu$ ).

$$\text{Rate} = \nu[X^\ddagger] = \nu[A][B]K^\ddagger \quad (7.21)$$

Since the rate of reaction is also

$$= k[A][B] \quad (7.22)$$

this leads to

$$k = \nu K^\ddagger \quad (7.23)$$

Although evaluation of  $k$  depends on our ability to deduce  $\nu$  and  $K^\ddagger$  this can be achieved via statistical mechanics to leave the result

$$k = k_B T/h K^\ddagger \quad (7.24)$$

where  $k_B$  on the right-hand side of the equation is the Boltzmann constant,  $T$  is temperature and  $h$  is Planck's constant. Equation 7.24 embodies thermodynamic quantities ( $\Delta G$ ,  $\Delta H$  and  $\Delta S$ ) since

$$\Delta G^\ddagger = -RT \ln K^\ddagger \quad (7.25)$$

and the rate constant can be expressed as

$$k = k_B T/h e^{-\Delta G^\ddagger/RT} \quad (7.26)$$

where  $\Delta G^\ddagger$  is the free energy of activation. Since the parameter  $k_B T/h$  is independent of A and B the rate of reaction is determined solely by  $\Delta G^\ddagger$ , the free energy of activation. Since

$$\Delta G^\ddagger = \Delta H^\ddagger - T\Delta S^\ddagger \quad (7.27)$$

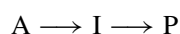


a thermodynamic formulation of transition state theory is often written as

$$k = k_B T / h e^{\Delta S^\ddagger / R} e^{-\Delta H^\ddagger / RT} \quad (7.28)$$

where  $\Delta S^\ddagger$  and  $\Delta H^\ddagger$  are the entropy and enthalpy of activation. For uncatalysed reactions reaching a transition state represents an enormous energy barrier to the formation of product. A large activation energy barrier is reflected by a slow reaction that arises because few reactants acquire sufficient thermal energy to cross this threshold.

Many reactions, particularly those in biological systems, consist of several steps. For reactions such as



the shape of the transition state diagram (Figure 7.5) reflects the overall reaction. If the activation energy of the first step ( $A \rightarrow I$ ) is greater than that of  $I \rightarrow P$  then the first step is slower than that of the second. The reaction with the highest activation energy represents the rate-determining step for the overall process.

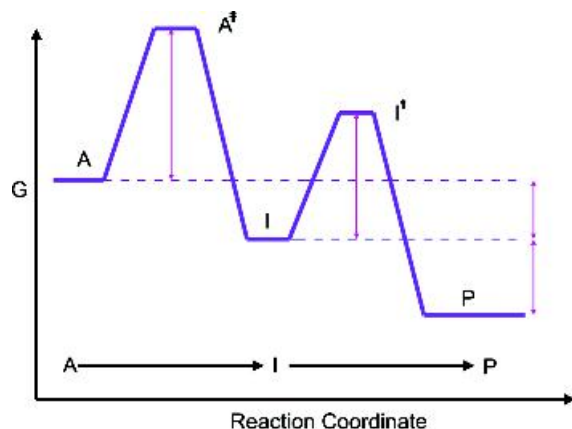


**Figure 7.5** Transition state diagram for a two-stage reaction where the step  $A \rightarrow I$  is the rate determining event. The shape of the transition barrier is described by 'box like' profiles (Figure 7.3), curves or gradients but these 2D representations are inaccurate since the pathway to the transition state is likely to be convoluted and reached by several 'routes'

Catalysts lower the energy associated with a transition state and increase the rate of a chemical reaction (termed velocity) without undergoing a net change over the entire process. The efficiency of a catalyst is reflected by lowering the activation energy with the difference in free energy ( $\Delta\Delta G^\ddagger$ ) allowing catalytic rate enhancements to be calculated ( $e^{-\Delta\Delta G^\ddagger / RT}$ ).

Enzymes are biological catalysts and increase the rate of a reaction of energetically favourable processes. As with all catalysts they are unchanged in chemical composition after a reaction. Enzymes produce dramatic rate enhancement as high as  $10^{15}$ -fold when catalysed and uncatalysed reactions are compared although normal ranges are from  $10^3$ – $10^9$ . Enzymes reduce the free energy of the transition state by promoting binding reactions that enhance intermediate stability. Enzymes employ a number of different mechanisms to achieve efficient catalysis. These mechanisms are influenced by the structure and dynamics of active site regions where environments differ significantly to those found in bulk solvent. Catalytic mechanisms identified within enzymes include acid–base catalysis, covalent catalysis, metal-ion mediated catalysis, electrostatic catalysis, proximity and orientation effects, and preferential binding of transition state complexes.

## The kinetics of enzyme action

In enzyme-catalysed reactions the concentration of catalyst is usually much lower than that of the substrate. As a result enzymes catalyse reactions several times, leading to relatively slow changes in the concentration of product and substrate whilst the concentration of enzyme can be viewed as constant. Early studies established kinetic principles through observation of the changes in concentration of substrate (or product) with time with the enzyme remaining an unobservable quantity. Often these changes were followed by spectrophotometric methods. For a simple enzyme-catalysed reaction (i.e. a reaction not involving allosteric modulators) it was recognized that as the concentration of substrate increased so the rate of appearance of product increased when the concentration of enzyme was held at a fixed level. However, at certain concentrations of substrate the rate of reaction no longer increased but reached a plateau (Figure 7.6).

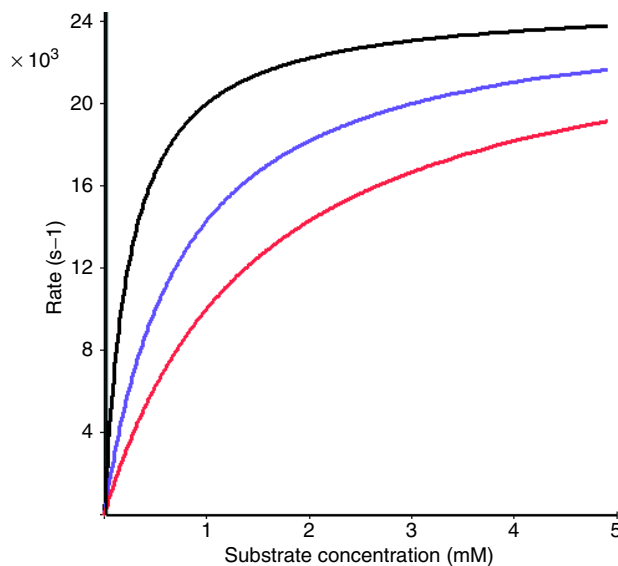


**Figure 7.6** Three different enzyme-catalysed reactions showing different  $K_m$  values but similar  $V_{max}$  values. See text for discussion of  $V_{max}$  and  $K_m$ . Each  $V_{max}$  is estimated from the asymptote approximating to the curve's maximum value and despite appearances these curves actually reach the same value at very high concentrations of substrate

The rate of reaction ( $v$ ) is proportional to the rate of removal of substrate or alternatively the rate of formation of product.

$$v = -d[S]/dt = d[P]/dt \quad (7.29)$$

At low substrate concentrations a linear or first order dependence on  $[S]$  exists whilst at higher substrate concentrations this shifts to zero order or substrate independent. The profile suggests that the enzyme-catalysed conversion of substrate into product involved the formation of an intermediate called the enzyme-substrate complex (Figure 7.7).

From a minimal reaction scheme, together with two assumptions originally formulated by Leonor Michaelis and Maud Menten, we can derive important enzyme

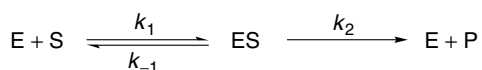


**Figure 7.7** The basic enzyme-catalysed reaction converts substrate into product

kinetic relationships. The two assumptions made by Michaelis and Menten were that the enzyme exists either as a free form  $[E]$  or as enzyme substrate complex  $[ES]$  and secondly that the enzyme substrate complex  $[ES]$  is part of an equilibrium formed between  $E$  and  $S$  during the time scale of the experiment or observation. These assumptions require that  $k_2$ , the rate of breakdown of the enzyme substrate complex, is much smaller than the remaining two rate constants. The total concentration of enzyme active sites ( $E_T$ ) is expressed as the sum of the free enzyme concentration ( $E$ ) plus that found in the enzyme substrate complex. The initial velocity of an enzyme-catalysed reaction is

$$v = -d[S]/dt = d[P]/dt = k_2[ES] \quad (7.30)$$

with a maximal velocity achieved at high substrate concentrations when the enzyme is saturated with substrate. Defining this maximal velocity as  $V_{max}$  leads to the following equalities

$$[ES] = [E_T] \Rightarrow V_{max} = k_2[E_T] = k_{cat}[E_T] \quad (7.31)$$

The enzyme substrate complex is called the Michaelis complex and the equilibrium formed with E and S is described by a constant called the Michaelis constant ( $K_m$ ). From the scheme above the Michaelis constant  $K_m$  is equal to

$$K_m = (k_2 + k_{-1})/k_1 = ([E_T] - [ES])[S]/[ES] \quad (7.32)$$

and since  $[E_T] - [ES] = [E]$  reorganization of this equation leads to

$$K_m[ES] = [E_T][S] - [ES][S] \quad (7.33)$$

$$K_mv/k_2 = V_{\max}/k_2[S] - v/k_2[S] \quad (7.34)$$

A final re-arrangement of the above equation leads to the velocity of an enzyme-catalysed reaction,  $v$ , expressed as a function of substrate concentration—the famous Michaelis–Menten equation

$$v = V_{\max}[S]/K_m + [S] \quad (7.35)$$

The velocity is related to substrate concentration through two parameters ( $V_{\max}$  and  $K_m$ ) that are specific and characteristic for a given enzyme under a defined set of conditions (pH, temperature, ionic strength, etc.). From the above equation it can be seen that when

$$[S] \ll K_m \quad v = V_{\max}[S]/K_m$$

$$\begin{aligned} [S] &\gg K_m & v &= V_{\max} \\ [S] &= K_m & v &= V_{\max}/2 \end{aligned} \quad (7.36)$$

The Michaelis–Menten equation is usually analysed by linear plots to derive the parameters  $K_m$  and  $V_{\max}$ . Most frequently used in enzyme kinetics is the Lineweaver–Burk plot of  $1/v$  versus  $1/[S]$  (Figure 7.8).

Although widely used the Lineweaver–Burk plot can be unsatisfactory because it fails to adequately define deviations away from linearity at high and low substrate concentrations. This problem can be neglected with the use of line fitting or linear regression analysis methods. More satisfactory in terms of data analysis is the Eadie–Hofstee plot where rearranging the Michaelis–Menten equation yields

$$v = -K_m v/[S] + V_{\max} \quad (7.37)$$

Experimental data are usually derived by measuring the initial velocity of the enzyme-catalysed reaction at a range of different substrate concentrations before substantial substrate depletion or product accumulation.

### **The steady state approximation and the kinetics of enzyme action**

An alternative approach to enzyme kinetic analysis proposed by G.E. Briggs and J.B.S. Haldane showed

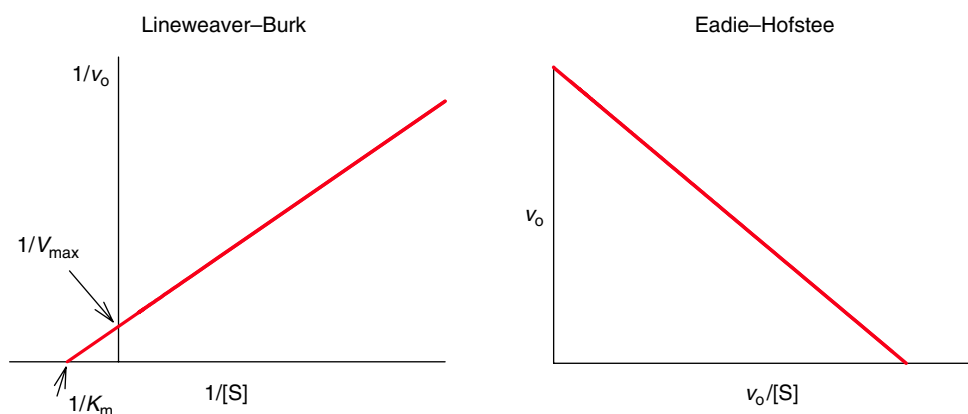


**Figure 7.8** Lineweaver–Burk and Eadie–Hofstee plots derived from the Michaelis–Menten equation. The slopes associated with each plot are  $K_m/V_{\max}$  and  $-K_m$  respectively

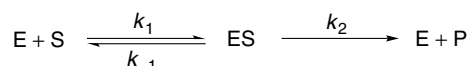


**Figure 7.9** The basic scheme for an enzyme-catalysed reaction

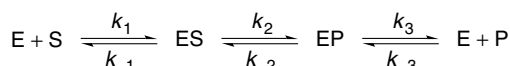


**Figure 7.10** A more detailed reaction scheme that describes an enzyme catalysed reaction

that it was unnecessary to assume that enzyme and substrate are in thermodynamic equilibrium with the ES complex (Figure 7.9).

After mixing together enzyme and substrate the concentration of ES rises rapidly reaching a constant level called the ‘steady state’ that persists until substrate depletion. Most rate measurements are made during the steady state period after the initial build up of ES called the pre-steady state and before substrate depletion. The ‘steady state approximation’ leads to the following relationships

$$d[ES]/dt = 0 = k_1[E][S] - (k_2 + k_{-1})[ES] \quad (7.38)$$

$$d[E]/dt = 0 = k_2 + k_{-1}[ES] - k_1[E][S] \quad (7.39)$$

The rate of formation of product is proportional to the concentration of ES

$$d[P]/dt = k_2[ES] \quad (7.40)$$

and from the steady state relationships defined above we have

$$k_1[E][S] = (k_2 + k_{-1})[ES] \quad (7.41)$$

This leads with the substitution of  $[E] = [E_T] - [ES]$  to

$$[E_T] = (k_2 + k_{-1})[ES]/k_1[S] + [ES] \quad (7.42)$$

$$= [ES](1 + (k_2 + k_{-1})/k_1[S]) \quad (7.43)$$

The Michaelis constant  $K_m$  is defined as  $(k_2 + k_{-1})/k_1$  and allows the above equation to be further simplified

$$[ES] = [E_T]/(1 + K_m/[S]) \quad (7.44)$$

Having defined the concentration of the ES complex we can now relate the formation of product ( $d[P]/dt$ ) to substrate concentration since

$$d[P]/dt = k_2[ES] = k_2[E_T]/(1 + K_m/[S]) \quad (7.45)$$

$$= k_2[E_T][S]/([S] + K_m) \quad (7.46)$$

A second assumption made in the Michaelis–Menten theory was that the enzyme exists in two forms: the enzyme and the enzyme–substrate complex. Observations derived from kinetic studies indicate several forms of enzyme–substrate complex and enzyme–product complex co-exist with the free enzyme. This allows the simple kinetic scheme to be redefined including reversible reactions and enzyme–product complex formed before product release (Figure 7.10).

$K_m$  is the initial substrate concentration that allows the reaction to proceed at the half maximal velocity.  $K_m$  is sometimes defined as the substrate dissociation constant ( $K_s = k_{-1}/k_1$ ) although this applies *only* under a restricted set of conditions when the catalytic constant  $k_{cat}$  is much smaller than either  $k_1$  or  $k_{-1}$ . Under these conditions, and only these conditions, the parameter  $K_m$  describes the affinity of an enzyme for its substrate.

$K_m$  discriminates between hexokinase and glucokinase; a rare example of two enzymes that catalyse the phosphorylation of glucose. The  $K_m$  for glucokinase is  $\sim 10$  mM whilst the  $K_m$  for hexokinase is  $\sim 100$   $\mu$ M. The  $K_m$  of each enzyme differs by a factor of  $\sim 100$  and although catalysing the same reaction these enzymes have different biological functions. Hexokinase is distributed throughout all cells and is the normal route for glucose conversion into glucose-6-phosphate. In contrast glucokinase is found in the liver and is used when blood glucose levels are high, for example after a carbohydrate-rich meal. It seems likely that enzymes possess  $K_m$  values reflecting intracellular levels of substrate to ensure turnover at rates close to maximal velocity.

More rigorous descriptions of enzyme activity involve the use of  $k_{cat}$  and  $K_m$ .  $K_m$  is a measure of the stability of the enzyme–substrate [ES] complex whilst  $k_{cat}$  is a first order rate constant describing the breakdown of the ES complex into

**Table 7.4** The efficiency of enzymes;  $k_{\text{cat}}/K_m$  ratios or specificity constants show a wide range of values

Enzyme	Substrate	$K_m$ (mM)	$k_{\text{cat}}$ ( $\text{s}^{-1}$ )	$k_{\text{cat}}/K_m$ ( $\text{M}^{-1} \text{s}^{-1}$ )
Carbonic anhydrase	$\text{CO}_2$	12.0	$1.0 \times 10^6$	$8.3 \times 10^7$
Catalase	$\text{H}_2\text{O}_2$	25.0	$4.0 \times 10^5$	$1.5 \times 10^7$
Pepsin	Phe-Gly of peptide chain	0.3	0.5	$1.7 \times 10^3$
Ribonuclease	$(\text{RNA})_n$	7.9	$7.9 \times 10^2$	$1.0 \times 10^5$
Tyrosyl-tRNA synthetase	tRNA	0.9	7.6	$8.4 \times 10^3$
Glucose isomerase	Glucose	140.0	$1.04 \times 10^3$	7.4
Fumarase	Fumarate	0.005	$8.0 \times 10^2$	$1.6 \times 10^8$
Lysozyme	$(\text{NAG-NAM})_3$	6	0.5	83
DNA polymerase I	dNTPs	0.025	1	$4.0 \times 10^4$
Acetylcholinesterase	Acetylcholine	0.095	$1.4 \times 10^4$	$1.5 \times 10^8$

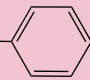
products. The magnitude of  $k_{\text{cat}}$  varies enormously with enzymes such as superoxide dismutase, carbonic anhydrase and catalase exhibiting high  $k_{\text{cat}}$  values ( $>10^5 \text{ s}^{-1}$ ) although values between  $10^2$ – $10^3$  are more typical of enzymes such as trypsin, pepsin or ribonuclease. By comparing the ratio of the turnover number,  $k_{\text{cat}}$ , to the  $K_m$  a measure of enzyme efficiency is obtained (Table 7.4). Some enzymes achieve high  $k_{\text{cat}}/K_m$  values by maximizing catalytic rates but others enzymes achieve high efficiency by binding substrate at low concentrations ( $K_m < 10 \mu\text{M}$ ).

Further insight into the significance of  $k_{\text{cat}}/K_m$  values is obtained by considering the Michaelis–Menten equation at low substrate concentration. Under conditions where  $[\text{S}] \ll K_m$  most of the enzyme is free and does not contain bound substrate, i.e.  $[\text{E}]_t \approx [\text{E}]$ . The equation becomes

$$v \approx k_{\text{cat}}/K_m[\text{E}][\text{S}] \quad (7.49)$$

The term  $k_{\text{cat}}/K_m$  is a second order rate constant for the reaction between substrate and free enzyme and is a true estimate of enzyme efficiency since it measures binding and catalysis under conditions when substrate and enzyme are not limiting. These values are particularly useful for comparing the efficiency of enzymes with different substrates. Proteolytic enzymes such as chymotrypsin show a wide range of substrate

**Table 7.5** The side chain preference of chymotrypsin in the hydrolysis of different amino acid methyl esters

Amino acid analogue	Side chain	$k_{\text{cat}}/K_m$
Glycine	—H	0.13
Norvaline	— $\text{CH}_2$ — $\text{CH}_2$ — $\text{CH}_3$	360
Norleucine	— $\text{CH}_2$ — $\text{CH}_2$ — $\text{CH}_2$ — $\text{CH}_3$	3000
Phenylalanine	— $\text{CH}_2$ — 	100 000

specificity, but measuring  $k_{\text{cat}}/K_m$  values for different substrates demonstrates a clear preference for cleavage of polypeptide chains after aromatic residues such as phenylalanine (Table 7.5). Using the amino acid methyl esters (Figure 7.11) as substrates the second order rate constant ( $k_{\text{cat}}/K_m$ ) is greater by a factor of  $\sim 10^7$  when the side chain is phenylalanine as opposed to glycine.

The  $k_{\text{cat}}/K_m$  ratio for enzymes such as fumarase, catalase, carbonic anhydrase and superoxide dismutase range from  $10^7$  to  $10^9 \text{ M}^{-1} \text{ s}^{-1}$  and are close to the diffusion-controlled limit where rates are determined

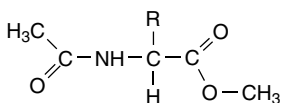


**Figure 7.11** A general structure for *N*-acetyl amino acid methyl esters

by diffusion through solution and all collisions result in productive encounters. For an average-sized enzyme this value is  $\sim 10^8\text{--}10^9\text{ M}^{-1}\text{ s}^{-1}$  and such reactions are said to be ‘diffusion controlled’. Many enzymes approach diffusion-controlled rates and molecular evolution has succeeded in generating catalysts of maximum efficiency. With knowledge about the kinetics and efficiency of enzymes it is relevant to look at the structural basis for enzyme activity yielding near perfect biological catalysts.

## Catalytic mechanisms

Why do enzymes catalyse reactions more rapidly and with higher specificity than normal chemical processes? Answering this question is the basis of understanding catalysis although it is interesting to note that biology employs exactly the same atoms and molecules as chemistry. Enzymes have ‘fine tuned’ catalysis by binding substrates specifically and with sufficient affinity in an active site that contains all functional groups. Enzymes are potent catalysts with ‘perfection’ resulting from a wide range of mechanisms that include acid–base catalysis, covalent catalysis, metal ion catalysis, electrostatic mechanisms, proximity and orientation effects and preferential binding of the transition state complex. To reach catalytic perfection many enzymes combine one or more of these mechanisms.

### Acid–base catalysis

Acid or base catalysis is a common method used to enhance reactivity. In acid-catalysed reactions partial proton transfer from a donor (acid) lowers the free energy of a transition state. One example of this reaction is the keto–enol tautomerization reactions (Figure 7.12) that occur frequently in biology. The

uncatalysed reaction is slow and involves the transfer of a proton from a methyl group to the oxygen via a high energy carbanion transition state.

Proton donation to the electronegative oxygen atom decreases the carbanion character of the transition state and increases rates of reaction whilst a similar effect is achieved by the proximity of a base and the abstraction of a proton. In biological reactions both processes can occur as concerted acid–base catalysis. Many reactions are susceptible to acid or base catalysis and in the side chains of amino acid residues enzymes have a wide choice of functional group. The side chains of Arg, Asp, Cys, Glu, His, Lys and Tyr are known to function as acid–base catalysts with active sites containing several of these side chains arranged around the substrate to facilitate catalysis.

Many enzymes exhibit acid–base catalysis although RNase A (Figure 7.13) from bovine pancreas is used here as an illustrative example. The digestive enzyme secreted by the pancreas into the small intestine degrades polymeric RNA into component nucleotides. Careful analysis of the pH dependency of catalysis of RNA hydrolysis observed two ionizable groups with  $pK_s$  of 5.4 and 6.4 that governed overall rates of reaction. Chemical modification studies suggested these groups were imidazole side chains of histidine residues. The active site of RNase A contains two histidines (12 and 119) with the side chains acting in a concerted fashion to catalyse RNA hydrolysis. A key event towards understanding mechanism was the observation that 2′–3′ cyclic nucleotides could be isolated from reaction mixtures indicating their presence as intermediates.

Hydrolysis is a two-step process; in the first stage His12 acts as a general base abstracting a proton from the 2′–OH group of the ribose ring of RNA. This event promotes nucleophilic attack by the oxygen on the phosphorus centre. His119 acts as an acid catalyst enhancing bond scission by donating a proton to the leaving group (the remaining portion of the polynucleotide chain) (Figure 7.14). The resulting 2′–3′ cyclic nucleotide is the identified intermediate. The cyclic intermediate is hydrolysed in a reaction where His119 acts as a base abstracting a proton from water whilst His12 acts as an acid. The completion of step 2 leaves the enzyme in its original state and ready to repeat the cycle for the next catalytic reaction.

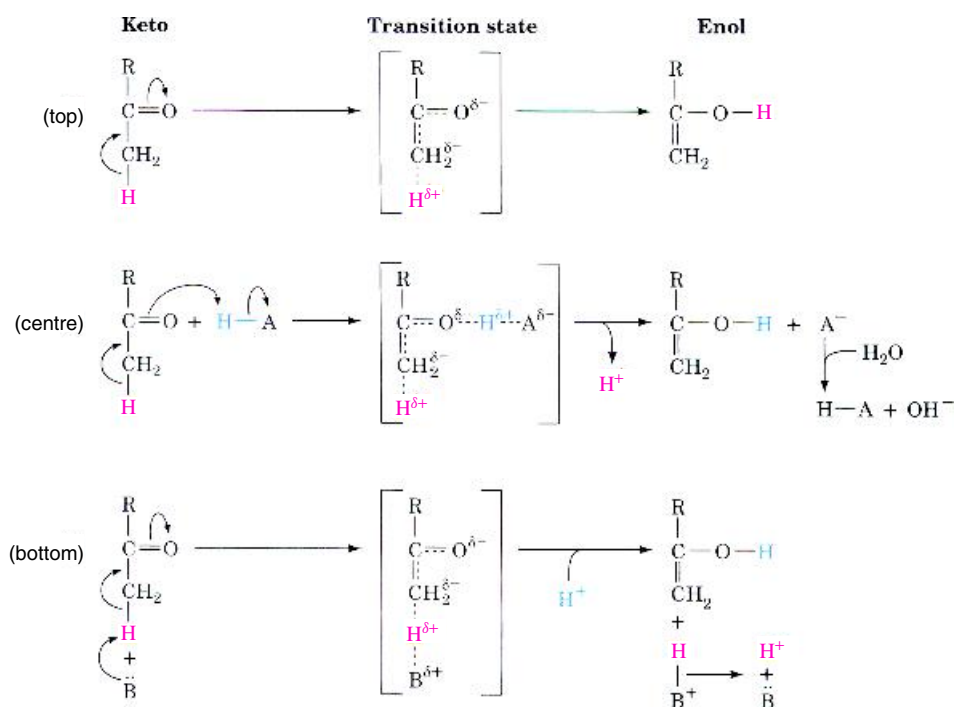


**Figure 7.12** Mechanism of keto-enol tautomerization. Top: uncatalysed reaction; centre: general acid-catalysed reaction; bottom: base-catalysed reaction. HA represents an acid B: represents a base. The transition state is enclosed in brackets to indicate 'instability'

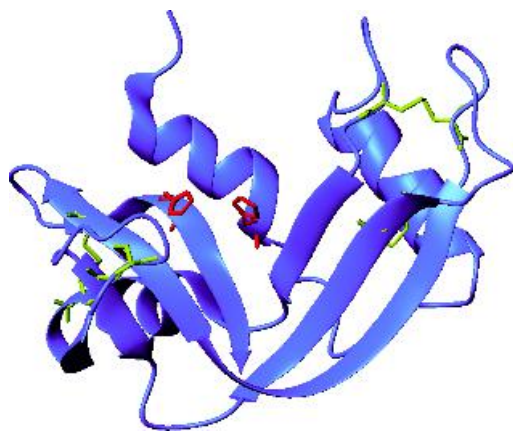


**Figure 7.13** The active site of RNase A within the protein structure. The enzyme is based predominantly around two collections of  $\beta$  sheet and four disulfide bridges (yellow). The active site histidines side are shown in red (PDB: 1FS3)

### Covalent catalysis

Transient formation of covalent bonds between enzyme and substrate accelerates catalysis. One method of achieving covalent catalysis is to utilize nucleophilic groups on an enzyme and their reaction with centres on the substrate. In enzymes the common nucleophiles are the oxygen of hydroxyl groups, the sulfur atom of sulphhydryl groups, unprotonated amines as well as unprotonated imidazole groups (Figure 7.15). The common link is that all groups have at least one set of unpaired electrons available to participate in catalysis.

Electrophiles include groups with unfilled shells frequently bonded to electronegative atoms such as oxygen. In substrates the most common electrophiles (Figure 7.16) are the carbon atoms of carbonyl groups although the carbon in cationic imine groups (Schiff base) are also relevant to catalysis.

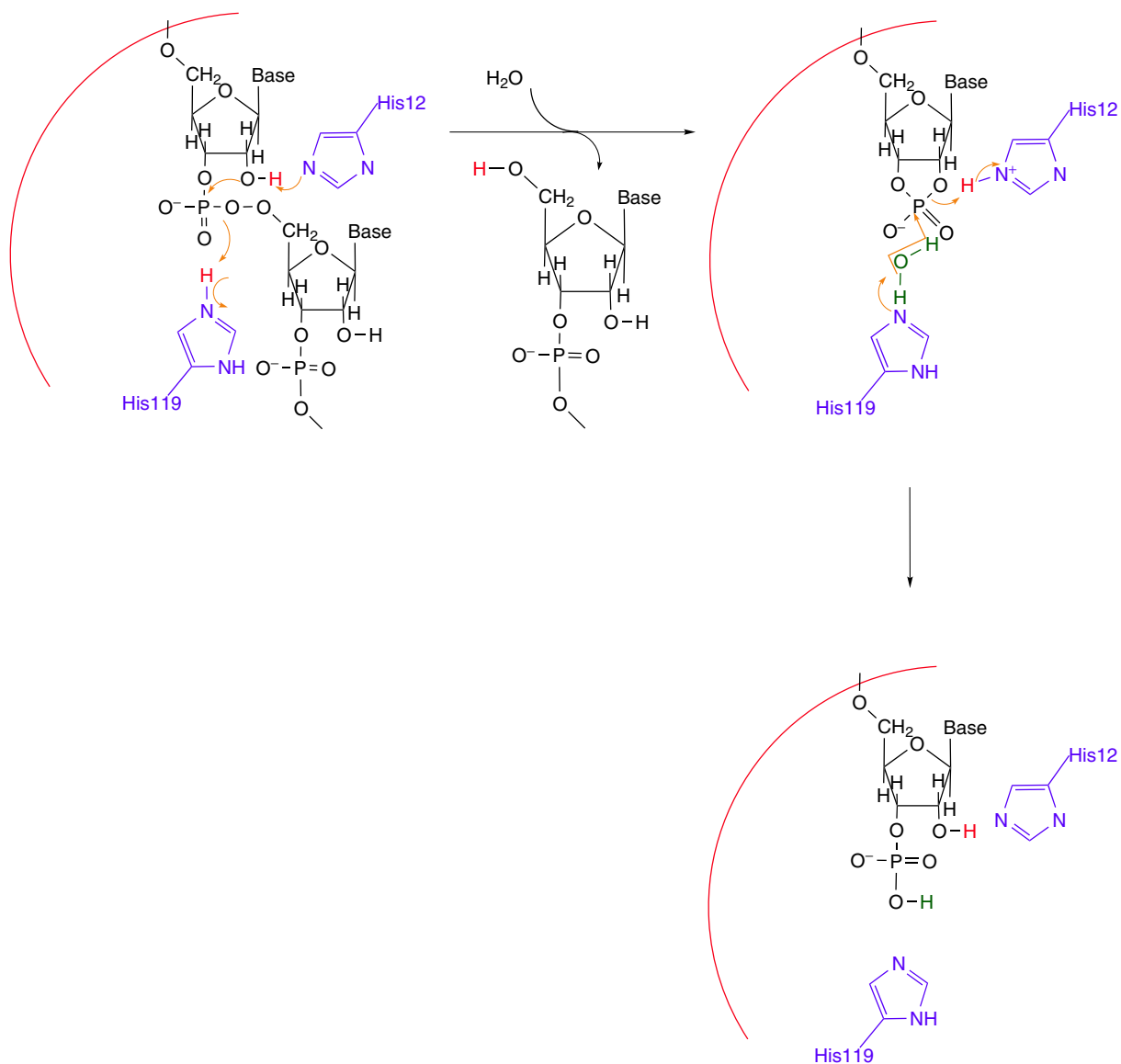
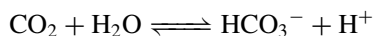


**Figure 7.14** The acid–base catalysis by His12 and His119 in bovine pancreatic RNaseA occurs in two discrete steps involving the alternate action of His12 first as a base and second as an acid. His119 acts in the opposite order

### **Metal ion catalysis**

Metalloenzymes use ions such as  $\text{Fe}^{2+}/\text{Fe}^{3+}$ ,  $\text{Cu}^+/\text{Cu}^{2+}$ ,  $\text{Zn}^{2+}$ ,  $\text{Mn}^{2+}$  and  $\text{Co}^{2+}$  for catalysis. Frequently, the metal ions have a redox role but additional important catalytic functions include directing substrate binding

and orientation via electrostatic interactions. Carbonic anhydrase, a zinc metalloenzyme found widely in cells (Figure 7.17), catalyses the reversible hydration of carbon dioxide





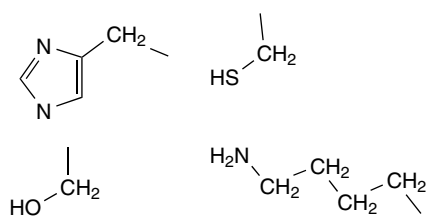


**Figure 7.15** Important nucleophiles found in proteins include the imidazole, thiol, amino and hydroxyl groups

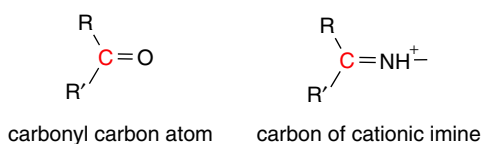


**Figure 7.16** Biologically important electrophilic groups

In red blood cells this reaction is of major importance to gaseous exchange involving transfer of  $\text{CO}_2$  from haemoglobin. At the heart of carbonic anhydrase is a divalent Zn cation essential for catalytic activity lying at the bottom of a cleft,  $\sim 1.5$  nm deep, coordinated in a tetrahedral environment to three invariant histidine residues and a bound water molecule. Enzyme kinetics show pH-dependent catalysis increasing at high pH and modulated by a group with a  $\text{p}K_a$  of  $\sim 7.0$ . Water molecules bound close to a metal ion tend to be stronger proton donors than bulk water with the result that in carbonic anhydrase the Zn not only orients the water at the active site but assists in base catalysis by removing a proton. This generates a bound hydroxide ion, a potent nucleophile, even at pH 7.0. This model is supported by the observation that anion addition inhibits enzyme activity by competing with  $\text{OH}^-$  anions at the Zn site.

At least 10 isozymes of carbonic anhydrase are identified in human cells with carbonic anhydrase II of particular pharmaceutical interest because its activity is linked to glaucoma via increased intra-ocular pressure. Uncontrolled increases in pressure in the eye damages the optic nerve leading to a loss of peripheral vision

and ‘blind spots’ in the field of sight. Drugs (enzyme inhibitors) combat glaucoma by binding to the active site. Acetazolamide, a member of the sulfonamide group of antibacterial agents, is the prototypal inhibitor and displaces the hydroxide ion at the Zn active site by ligation through the ionized nitrogen of the primary sulfonamide group (Figure 7.18).

### Electrostatic catalysis

Substrate binding to active sites is often mediated via charged groups located in pockets lined with hydrophobic side chains. Any charged side chain located in this region will exhibit a  $\text{p}K_a$  shifted away from its normal ‘aqueous’ value and exhibits in theory at least, a massive potential for electrostatic binding and catalysis. Direct involvement of charged residues in catalysis has proved harder to demonstrate, in contrast to many studies showing that substrate binding is enhanced by charge distribution. The aim of electrostatic catalysis is to use the distribution of charged groups at the active site of enzymes to enhance the stability of the transition state. This aspect of electrostatic enhancement of catalysis has been termed the ‘circe’ effect by W.P. Jencks and encompasses the use of attractive forces to ‘lure’ the substrate into the active site destabilizing the reactive group undergoing chemical transformation.

Orotidine 5'-monophosphate decarboxylase (ODCase) catalyses the conversion of orotidine 5'-monophosphate to uridine 5'-monophosphate, the last step in the biosynthesis of pyrimidine nucleotides (Figure 7.19). ODCase catalyses exchange of  $\text{CO}_2$  for a proton at the C6 position of uridine 5'-monophosphate in a reaction that is exceptionally slow in aqueous solution but is accelerated 17 orders of magnitude by enzyme. The mechanism underlying enhancement has fascinated chemists and biochemists alike and in the active site of the  $\beta$  barrel are a series of charged side chains (Lys42-Asp70-Lys72-Asp75) found close together. Although definitive demonstration of the role of these residues in the activity of ODCase requires further study the frequent presence of charge groups in non-polar active sites points to the involvement of electrostatics in catalysis.

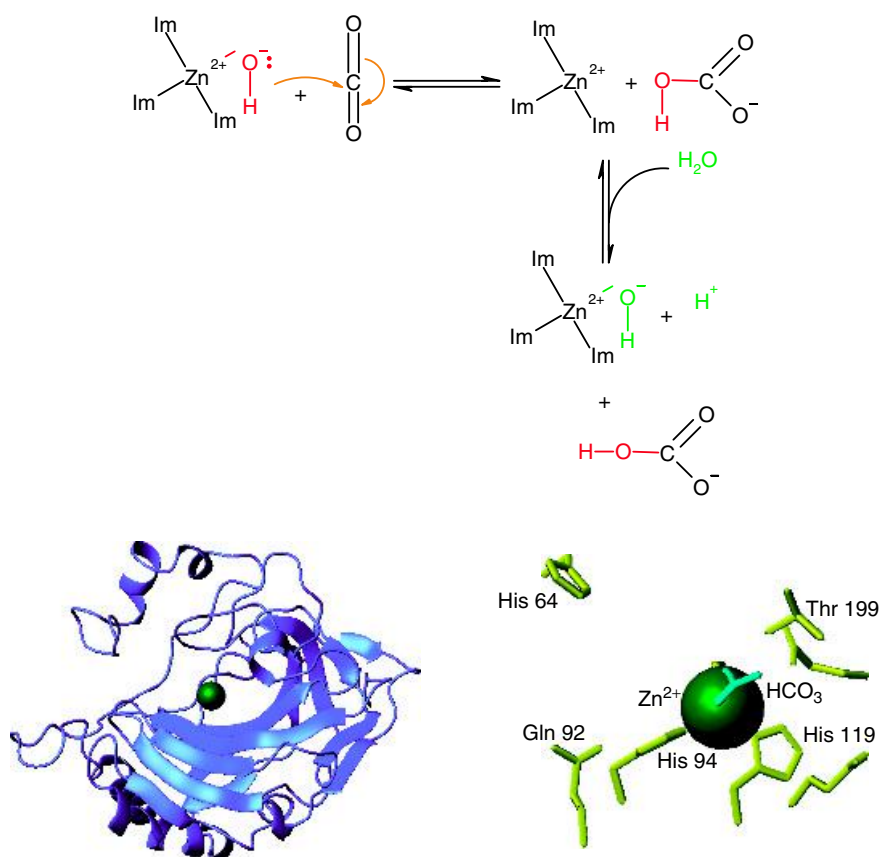


**Figure 7.17** The arrangement of imidazole ligands (Im) around the central Zn cation in carbonic anhydrase favours abstraction of a proton from water and the nucleophilic attack by the hydroxide ion on carbon dioxide bound nearby. The imidazole ligands arise from His 94, His96 (hidden by Zn), and His119. A zinc bound hydroxide ion is hydrogen bonded to the hydroxyl side chain of Thr199, which in turn hydrogen bonds with Glu106. Catalytic turnover requires the transfer of the product proton to bulk solvent via shuttle groups such as His64. Shown in the diagram of the active site is the bicarbonate ion bound to the zinc

### **Catalysis through proximity and orientation effects**

Biological catalysis is typified by high specificity coupled with remarkable speed. The gains in efficiency for enzyme-catalysed reactions arise from specific environments found at active sites that promote chemical reactions to levels of efficiency the organic chemist can only dream about. Two parameters that are important in modulating catalysis are proximity and orientation.

These superficially nebulous terms include the effects of binding substrates close to specific groups thereby facilitating chemical reactions coupled with the binding of substrate in specific, restrictive, orientations.

The potential effects of proximity on rates of reaction have been demonstrated through experiments involving the non-enzymatic hydrolysis of *p*-bromophenylacetate. The reaction is first performed as a simple bimolecular reaction and compared with a series of intramolecular reactions in which the

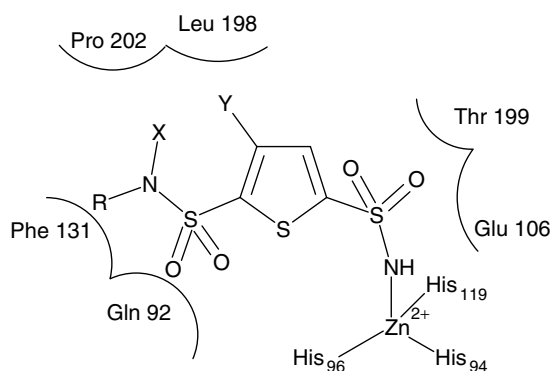


**Figure 7.18** General scheme of sulfonamide inhibitor binding to carbonic anhydrase. The 'primary sulfonamide' coordinates to the active site zinc ion and hydrogen bonds with Thr199

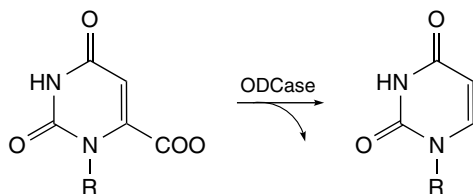


**Figure 7.19** The reaction catalysed by orotidine 5'-monophosphate decarboxylase converts orotidine 5'-monophosphate into uridine monophosphate in the final step in pyrimidine biosynthesis. R is a ribose 5'-phosphate group in both reactant and product

reacting groups are connected by a bridge that exerts progressively more conformational restriction on the molecule. In the simple bimolecular reaction *p*-bromophenylacetate is hydrolysed to yield bromophenolate anion with the formation of acetic anhydride (Figure 7.20). The rate of hydrolysis of bromophenol esters increases dramatically as the reactants are held in closer proximity and in restricted conformations. The relative rate constants increase from 1 (on an arbitrary scale) to  $10^3$ , to  $10^5$  and finally in the most restricted form to a value approaching  $10^8$  times

greater than that exhibited by the bimolecular reaction. Although the unimolecular reactions described here do not involve true catalysis they emphasize the significant rate enhancement that results from controlling proximity and orientation. The intramolecular reactions model the binding and positioning of two substrates within an enzyme active site and although sizeable rate enhancements occur they do not account for all of the observed increase in rates seen in enzyme versus uncatalysed reactions (for example orotidine 5'-monophosphate decarboxylase enhances rates  $\sim 10^{17}$ -fold). Enzymes have yet further mechanisms to enhance catalysis.

### *Preferential binding of the transition state causes large rate enhancements*

Acid–base catalysis and covalent catalytic mechanisms can perhaps enhance rates by factors of  $10$ – $10^2$  whilst proximity and orientation can achieve enhancements of up to  $10^8$ , although frequently it is much less. To achieve the magnitude of catalytic enhancement seen for some enzymes additional mechanisms are required to achieve the ratios of  $10^{14}$ – $10^{17}$  seen for urease, alkaline phosphatase and ODCase. One of the most important catalytic mechanisms exhibited by enzymes is the ability to bind transition states with greater affinity than either products or reactants.

For many organic reactions the concept of strain is well known and it would not be surprising if enzymes adopted similar mechanisms. Enzymes are envisaged as 'straining' or 'distorting' their substrates towards the transition state geometry by the formation of binding sites that do not allow productive binding of 'native' substrates. Thus, the rate of a catalysed reaction compared with an uncatalysed one is related to the magnitude of transition state binding. Catalysis results from preferential transition state binding or the stabilization of the transition state relative to the substrate. In this manner a rate enhancement of  $10^6$  would require a  $10^6$  enhancement in transition state binding relative to that of the substrate. This corresponds at room temperature (298 K) to an increased binding affinity of  $\sim 34$  kJ mol $^{-1}$ . In terms of bond energies this is the

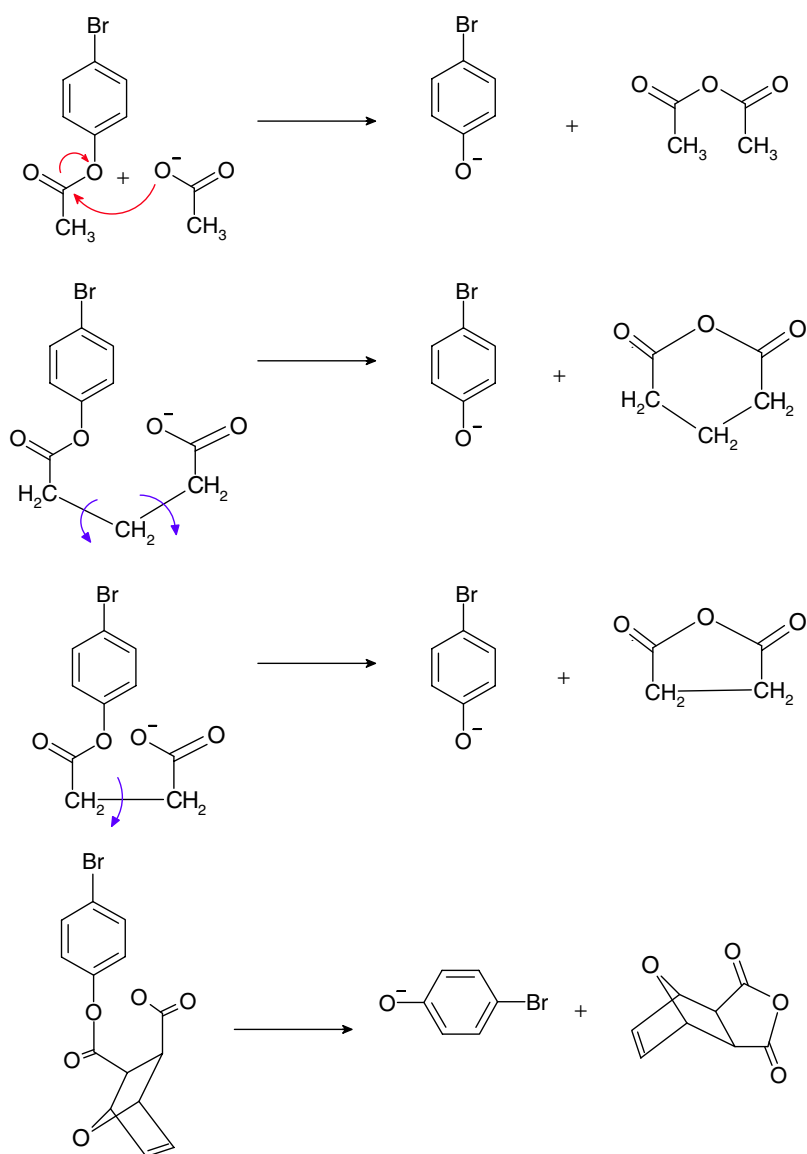


**Figure 7.20** Bimolecular and unimolecular reactions describing the hydrolysis of bromophenol esters. The reactions illustrate how proximity effects enhance catalysis. A progressive increase in rate constant occurs from a relative value of 1 in the top reaction to  $10^3$ ,  $10^5$  and finally  $10^8$

equivalent of a handful of hydrogen bonds. Very large rate enhancements will result from the formation of new bonds between transition state and enzyme and this mechanism underpins rate enhancement by enzymes. Additional bonds can involve non-reacting regions

of the substrate and many proteolytic enzymes show substrate specificity that depends on residues bordering the scissile bond at the  $P_4, P_3$  subsites, for example. The concept of transition state binding also explains why some enzymes bind substrates with acceptable



**Figure 7.21** Conversion of dihydroxyacetone phosphate (DHAP) into glyceraldehyde-3-phosphate (G3P) by triose phosphate isomerase

affinity but fail to show significant catalytic enhancement. These ‘poor’ substrates do not form transition states and hence do not exhibit high turnover rates. As a corollary it is not accurate to say that enzymes bind substrates with the highest affinity – this is reserved for transition state complexes.

The concept of transition state binding receives further support from the observation that transition state analogues, stable molecules that resemble the transition state, are potent catalytic inhibitors. Many transition state analogues are known and used as enzyme inhibitors. 2-Phosphoglycolate is an inhibitor of triose phosphate isomerase. The reaction (Figure 7.21) involves general acid–base catalysis and the formation of enediol/enediolate intermediates (Figure 7.22). 2-Phosphoglycolate resembles the intermediate and was observed to bind to the enzyme with greater affinity than either dihydroxyacetone phosphate or glyceraldehyde-3-phosphate. Increased binding arises from the partially charged oxygen atom

found on 2-phosphoglycolate and the transition state but not on either substrate.

## Enzyme structure

One of the prime reasons for wanting to determine the structure of enzymes is to verify different catalytic mechanisms. In many instances structural description of enzymes refines or enhances particular catalytic schemes, whilst in a few cases it has dictated a fresh look into enzyme mechanism.

## Lysozyme

No discussion of enzyme structure would be complete without a description of lysozyme, a hydrolytic enzyme or hydrolase. It destroys bacterial cell walls by hydrolysing the  $\beta(1\rightarrow4)$  glycosidic bonds between *N*-acetylglucosamine (NAG) and *N*-acetylmuramic acid (NAM) that form the bulk of peptidoglycan cell walls (Figure 7.23). It will also hydrolyse poly-NAG chains

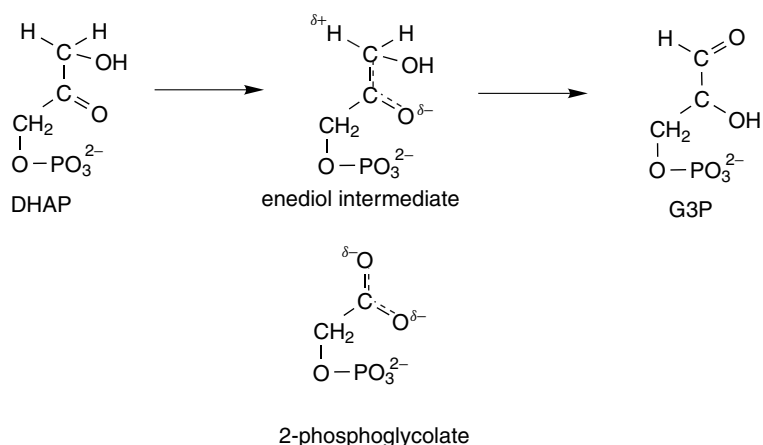


**Figure 7.22** The first enediol intermediate in the conversion of dihydroxyacetone phosphate (DHAP) into glyceraldehyde-3-phosphate (G3P) and the structure of 2-phosphoglycolate, a transition state analogue and an inhibitor of triose phosphate isomerase

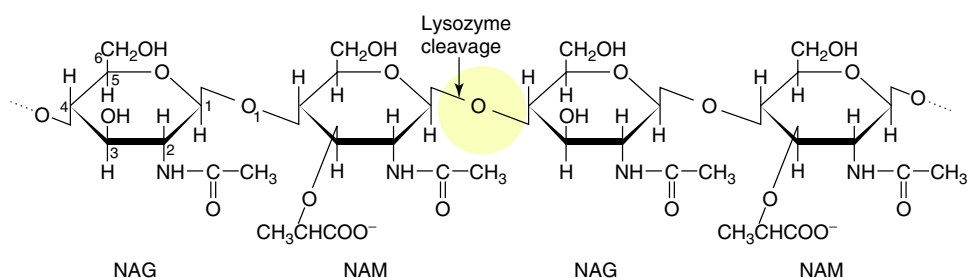


**Figure 7.23** The lysozyme cleavage site after the  $\beta(1\rightarrow4)$  linkage in alternating NAG–NAM units of the polysaccharide components of cell walls. Reproduced from Voet *et al.* (1998) by permission of John Wiley & Sons, Ltd. Chichester

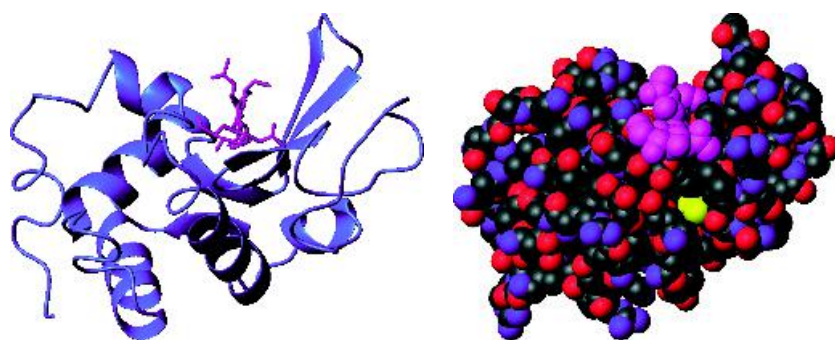


**Figure 7.24** The three-dimensional structure of lysozyme (PDB: 1HEW). The distribution of secondary structure is shown together with the binding of a poly-NAG trimer. A space filling model from the same view emphasizes the cleft into which the polysaccharide, shown in magenta, fits precisely. The cleft can accommodate six sugar units

such as those in chitin a key extracellular component of fungal cell walls and the exoskeletons of insects and crustaceans.

The structure of lysozyme determined by David Phillips in 1965 represented the first three-dimensional structure for an enzyme (Figure 7.24). The protein was elliptical in shape ( $3.0 \times 3.0 \times 4.5$  nm), with the most striking feature being a prominent cleft that traversed one face of the molecule. Although a picture of substrate binding sites had been established from kinetic and chemical modification studies this feature provided a potent image of 'active sites'. Lysozyme contains five helical segments together with a triple stranded anti-parallel  $\beta$  sheet that forms one wall of the binding site for NAG–NAM polymers and a smaller  $\beta$  strand region. Models of lysozyme complexed with saccharides reveal a cleft accommodating six units at

individual sites arranged linearly along the binding surface. The sites are designated A–F; NAM binds to sites B, D and F because there is not enough space for the bulkier side chains at positions A, C and E. The remaining sites are occupied by NAG.

Sites B and F accommodate NAM without distortion but at site D the sugar molecule will only fit with distortion from its normal chair conformation into a half-chair arrangement (Figure 7.25). Moreover, trimers of NAG bound at sites A–C are not hydrolysed at significant rates, and by performing lysozyme-mediated catalysis in the presence of  $\text{H}_2\text{O}^{18}$  it was demonstrated that hydrolysis occurred between the  $\text{C}_1$  and O atoms of the glycosidic bond located at subsites D and E (Figure 7.26). At this site two side chains from Glu35 and Asp52 are located close to the  $\text{C}_1$  position of the distorted sugar. These two side chains are the

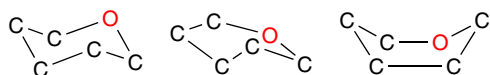


**Figure 7.25** Chair, half chair and boat conformations for hexose sugars

only potential catalytic groups in the vicinity of the target C–O bond.

Glu35 is located in a non-polar environment and has an elevated  $pK_a$  of  $\sim 6.5$ . Asp52 in contrast has a more typical value around 3.5. The pH optimum for lysozyme is 5.0, midway between the  $pK_a$ s associated with each of these side chains. Glu35, as a result of its unusual  $pK$ , is protonated at pH 5.0 and acts as an acid catalyst donating a proton to the oxygen atom involved in the glycosidic bond between the D and E sites (Figure 7.27). Cleavage occurs and a portion of

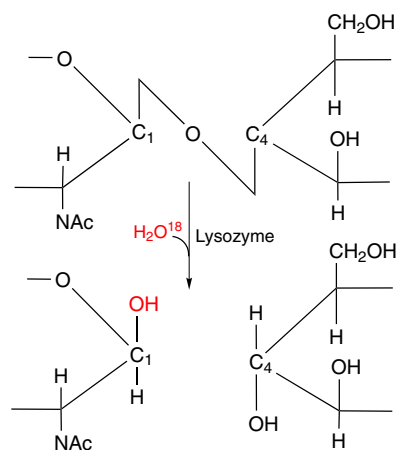


**Figure 7.26** Hydrolysis of NAM–NAG polymers by lysozyme in the presence of  $^{18}\text{O}$ -labelled  $\text{H}_2\text{O}$

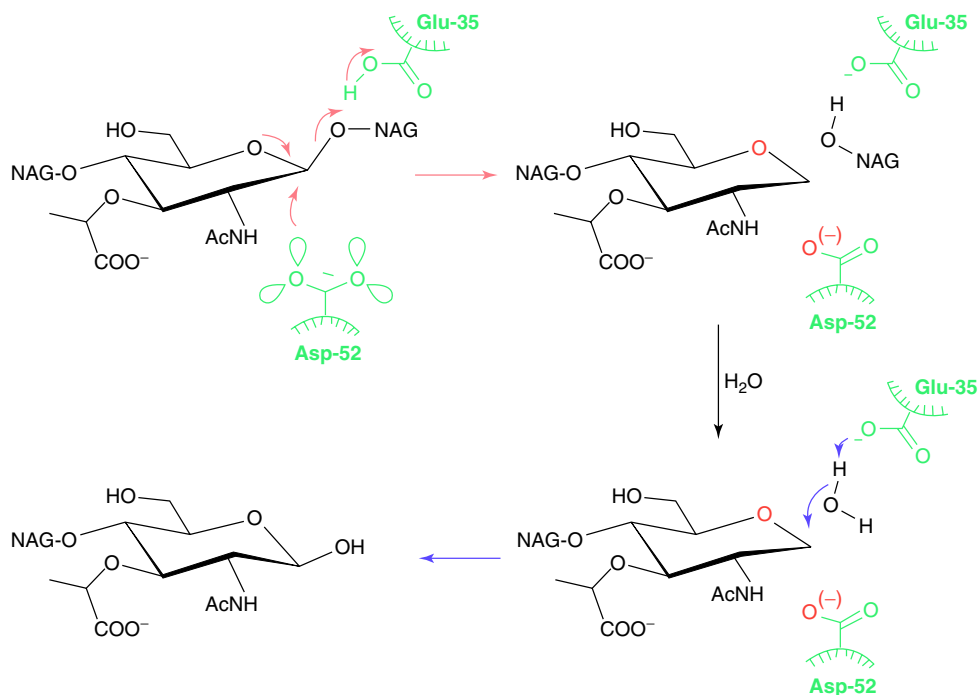


**Figure 7.27** The hydrolysis of NAG–NAM polysaccharides catalysed by lysozyme. The substrate is bound so that the leaving group oxygen, the 4-OH group of an *N*-acetylglucosamine (NAG) residue, is protonated as it leaves via the COOH group of Glu35. High  $pK$  favours protonation. Enzyme groups are coloured green (reproduced with permission from Kirby, A.J. *Nature Struct. Biol.* 2001, **8**, 737–739. Macmillan)

the substrate bound at sites E and F can diffuse out of the cleft to be replaced by water. The resulting cleavage leads to the formation of a carbocation which interacts with the carboxylate group of Asp 52 (nucleophile) to form a glycosyl–enzyme intermediate in a concerted  $S_N2$ -type reaction. The carboxylate group is then displaced from the glycosyl–enzyme intermediate by a water molecule that restores the original configuration at the  $C_1$  centre.

## The serine proteases

The serine proteases include the common proteolytic enzymes trypsin and chymotrypsin, as well as acetylcholinesterase, an enzyme central to the transmission of nerve impulses across synapses, thrombin (an enzyme with a pivotal role in blood coagulation) and elastase (a protease important in the degradation of connective fibres). As proteases these enzymes hydrolyse peptide bonds in different target substrates but are linked by the presence of an invariant serine residue at the enzyme active site that plays a pivotal role in catalysis.

For trypsin, chymotrypsin, elastase and thrombin the enzymes cut polypeptides on the C-terminal side of specific residues. These residues are not random

but show a substrate specificity that differs widely from one enzyme to another. Trypsin cuts preferentially after positively charged side chains such as arginine or lysine whilst chymotrypsin shows a different specificity cutting after bulking hydrophobic residues with a clear preference for phenylalanine, tyrosine, tryptophan and leucine. In contrast, elastase cuts only after small and neutral side chains whilst thrombin shows a restricted specificity for arginine side chains (Figure 7.28). The substrate specificity arises from the properties of the active site pocket and in particular the identity of residues at subsites making up the substrate binding region. The subsites that bind substrate residues preceding the scissile bond are termed S1, S2, S3, whilst those after this bond are given the names S1', S2', S3', etc. A similar terminology is applied to the peptide substrate where P3, P2 and P1 sites precede the scissile bond and P1', P2', and P3' continue after it.

Serine proteases show similar structures with the active site containing three invariant residues arranged in close proximity. These residues are His57, Asp102 and Ser195 and together they form a catalytic triad linked by a network of hydrogen bonds. In addition to these three invariant residues the serine proteases possess a pocket, located close to the active site serine that strongly influences substrate specificity. In trypsin the pocket is relatively long and narrow with a strategically located carboxylate side chain found at the bottom of the pocket. In view of the preferred specificity of trypsin for cleavage after lysine or arginine side chains this pocket appears to have been tailored to ‘capture’ the substrate very effectively. In chymotrypsin the pocket is larger, wider, lacks charged residues but contains many hydrophobic groups. This is consistent with specificity towards bulky aromatic groups. Elastase, in contrast, has a shallower pocket formed by valine and threonine side chains. Its specificity for cleavage on the C-terminal side of small, uncharged, side chains again reflects organization of the pocket.

Despite tailoring substrate specificity through the properties of the pocket all serine proteases show similar catalytic mechanisms based around a highly reactive serine residue identified from labelling and chemical inactivation studies. Agents based around organophosphorus compounds such as di-isopropylphosphorofluoridate (DIPF) were identified via their action as potent neurotoxins (Figure 7.29). Neurotoxicity arises

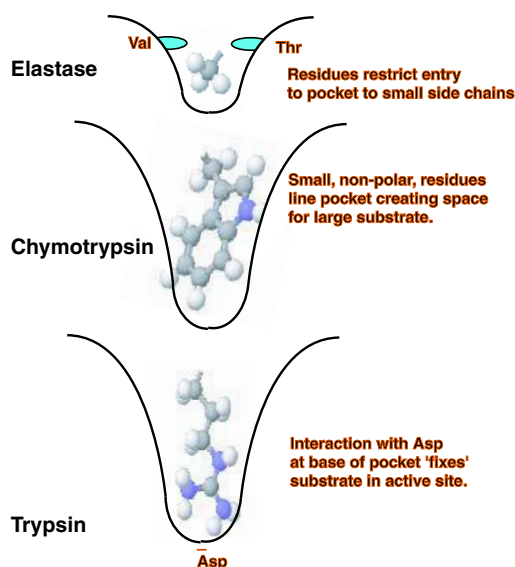


**Figure 7.28** Representation of substrate specificity pockets for elastase, chymotrypsin and trypsin



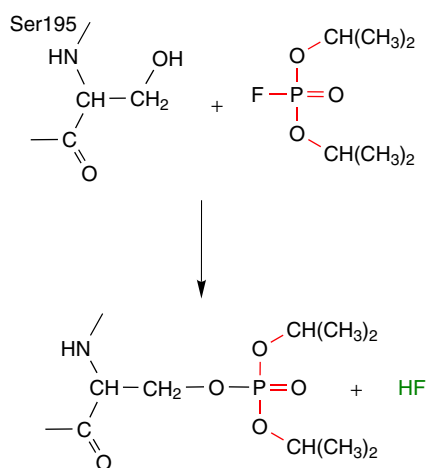


**Figure 7.29** Inactivation of serine proteases by diisopropylphosphorofluoridate with the formation of DIP-enzyme

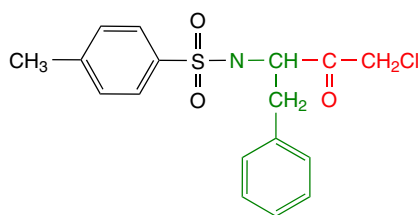


**Figure 7.30** Tosyl-L-phenylalanine chloromethylketone (TPCK)

from modification of an active site serine residue in acetylcholinesterase and indicated the similarity of this enzyme to other serine proteases such as trypsin and chymotrypsin where DIPF covalently reacts with Ser195 to form an adduct lacking catalytic activity. Labelling studies also identified the importance of a second residue of the catalytic triad, His57. Chymotrypsin binds tosyl-L-phenylalanine chloromethylketone (TPCK, Figure 7.30) as a result of the presence of a phenyl group, a preferred substrate, within the analogue. The reactive group forms a stable covalent bond with the imidazole side chain (Figure 7.31).

The structure of chymotrypsin revealed the close proximity of His57 and Ser195 together with Asp102 in the active site despite their separation in the primary

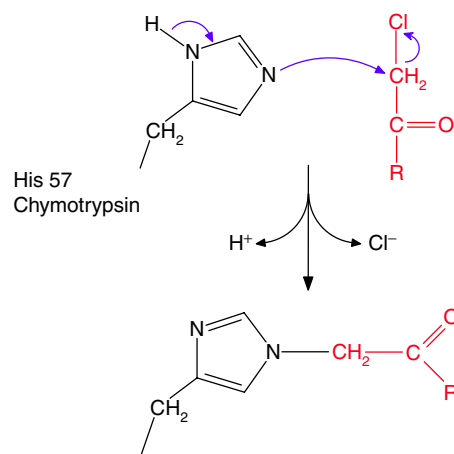


**Figure 7.31** The reaction of TPCK with His57 of chymotrypsin. Only the active part of TPCK is shown (red)- alkylation causes enzyme inactivation

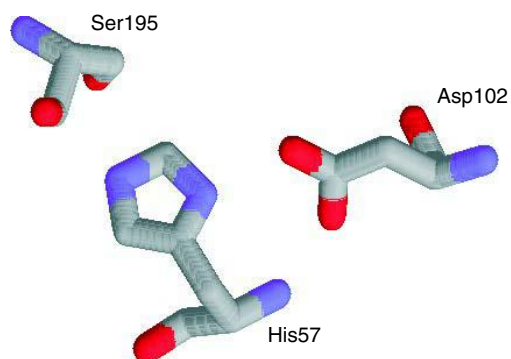


**Figure 7.32** The spatial arrangement of residues in the catalytic triad (His57, Asp102 and Ser195) in the active site of chymotrypsin (PDB: 2CGA)

sequence (Figure 7.32). The first step of catalysis is substrate binding to the active site region and specificity is largely dictated by residues at the bottom of a well-defined cleft. Interactions at subsites either side of the scissile bond are limited. Specific binding leads to close proximity between Ser195 and the carbonyl group of the bond to be cleaved. Under normal conditions the  $pK_a$  of the  $-OH$  group of serine is very high ( $>10$ ) but in chymotrypsin the proximity of His57 leads to proton transfer and formation of

a charged imidazole group. Protonation of His57 is further stabilized by the negative charge associated with Asp102 – the third member of the catalytic triad – that lies in a hydrophobic environment. The formation of a strong nucleophile in the activated serine attacks the carbonyl group as the first step in peptide bond cleavage. Nucleophile generation

is triggered by small conformational changes upon substrate binding that cause Asp102 and His57 to form a hydrogen bond. The influence of this hydrogen bond raises the  $pK$  of the imidazole side chain from  $\sim 7$  to  $\sim 11$  increasing its basicity. Electrons driven towards the second nitrogen atom form a stronger base that abstracts a proton from the normally

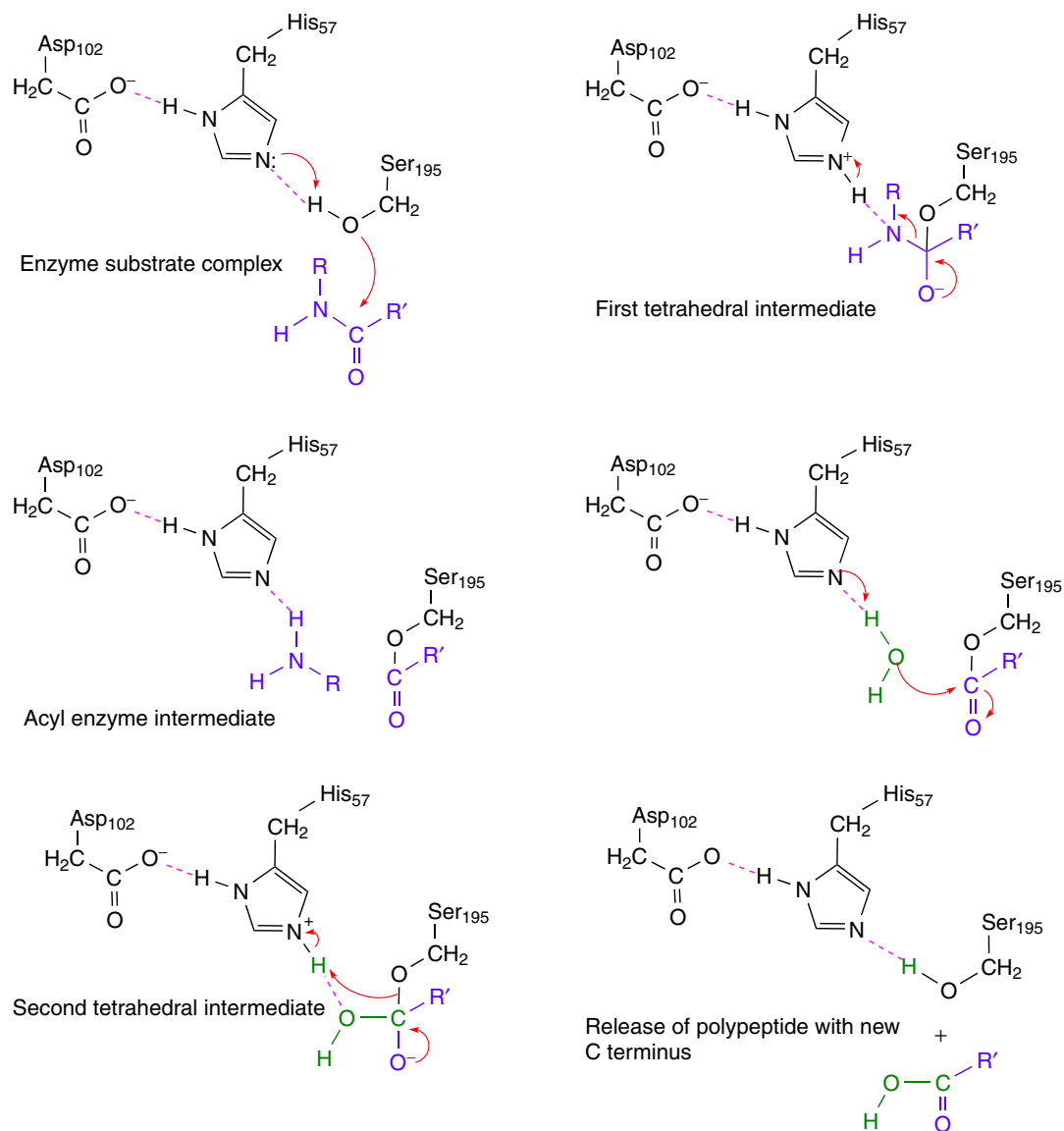


**Figure 7.33** The catalytic cycle of serine proteases such as chymotrypsin

unreactive side chain of Ser195 creating the potent nucleophile.

Nucleophilic attack results in a tetrahedral transition state followed by cleavage of the peptide bond. The N-terminal region of the peptide substrate remains covalently linked to the enzyme forming an acyl enzyme intermediate. The proton originally attached to the serine residue and located on the histidine is abstracted by the C-terminal peptide to form a new terminal amino group and this region of the peptide does not bind strongly to the enzyme. As a hydrolytic enzyme, water is involved in the overall reaction summarized in Figure 7.33.

In chymotrypsin water displaces C-terminal peptide from the active site and hydrolyses the acyl-enzyme intermediate. The water molecule donates a proton to the imidazole side chain and forms a second tetrahedral transition state with the acyl intermediate. This intermediate is hydrolysed as a result of proton transfer from His57 back to Ser195 with restoration of the active site to its original state with the release of the N-terminal peptide. Serine proteases follow a ping-pong mechanism (Figure 7.34); the substrate is first bound to the enzyme, the C-terminal peptide is released followed by binding a water molecule and the formation of an acyl-enzyme intermediate. This is completed by release of the N-terminal peptide from hydrolysis of the acyl-enzyme

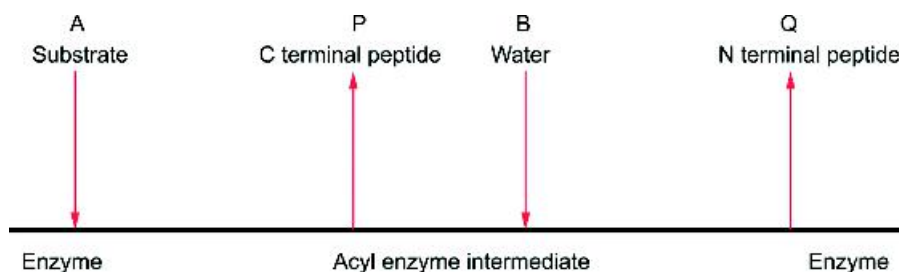
intermediate. The type of group transfer where one or more products are released before all substrates are added is also known as a double-displacement reaction.

It is interesting to note that serine proteases utilize the whole gamut of catalytic mechanisms. Proximity effects play a role in generation of the bound substrates whilst transition state stabilization ensures effective binding prior to catalysis. This is complemented by the use of covalent catalysis (the serine nucleophile) together with acid–base catalysis by histidine to yield efficient enzyme action.

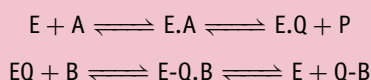
### Triose phosphate isomerase

Triose phosphate isomerase has been widely studied and catalyses the conversion between DHAP and G3P (Figure 7.35). The equilibrium for the reaction lies in favour of DHAP, but the rapid removal of G3P by successive reactions in glycolysis drives the reaction towards the formation of G3P.

Triose phosphate isomerase merits further discussion as an example of enzyme catalysis because of two interesting phenomena: the use of the imidazolite form of histidine in catalysis and the evolution of the enzyme towards a near perfect biological catalyst. Influencing both of these phenomena is the structure of triose phosphate isomerase with crystallographic structures



**Figure 7.34** The ping-pong mechanism for serine proteases. Using the normal convention A and B represent substrates in the order that they are bound by the enzyme whilst P and Q represent products in the order that they leave the enzyme. The activity of trypsin and other serine proteases are therefore summarized by a scheme



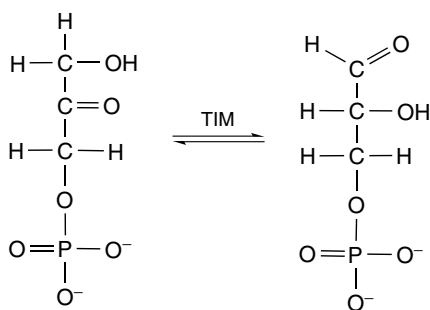


**Figure 7.35** The interconversion of dihydroxyacetone phosphate (left) and glyceraldehyde-3-phosphate catalysed by triose phosphate isomerase

of the enzyme available in a free state, bound with DHAP and plus 2-phosphoglycolate. Kinetic studies on the pH dependence of the catalytic process revealed two inflection points in the profile corresponding to pH values of  $\sim 6.0$  and  $9.0$ . When considered alongside the structure of triose phosphate isomerase (Figure 7.36) these values implicated the side chains of glutamate and histidine. Affinity labelling studies using bromohydroxyacetone phosphate modified a glutamate residue within a hexapeptide (Ala-Tyr-Glu-Pro-Val-Trp) and this residue was identified as Glu165. The

active site lies near the top of the  $\beta$  barrel with Glu165 close to His 95 as well as Lys12, Glu97 and Tyr208. Both Glu165 and His 95 are essential for catalytic activity and the enzyme provides a cage or reaction vessel holding substrate and protecting intermediates through a series of 11 residues immediately after Glu165 (residues 166–176) that form a loop and acts as a lid for the active site.

Dihydroxyacetone phosphate binds to the active site with the carbonyl oxygen forming a hydrogen bond with the neutral imidazole side chain of His95. The glutamate side chain is charged and facilitates abstraction of a proton from the C1 carbon of dihydroxyacetone phosphate. In this state the His95 forms a strong hydrogen bond with the carbonyl oxygen (C2) of the enediolate intermediate that leads to protonation of this atom. Protonation of the oxygen atom forms an imidazolium side chain on His95 that has a positive charge and is a strong base. Proton abstraction from the hydroxyl group attached to the C1 carbon results in the formation of a second enediolate intermediate with this unstable intermediate converted to the final product by donation of a proton from Glu165 to the C2 carbon. These reactions are shown in Figure 7.37.

Kinetic and thermodynamic characterization of triose phosphate isomerase show measurable binding

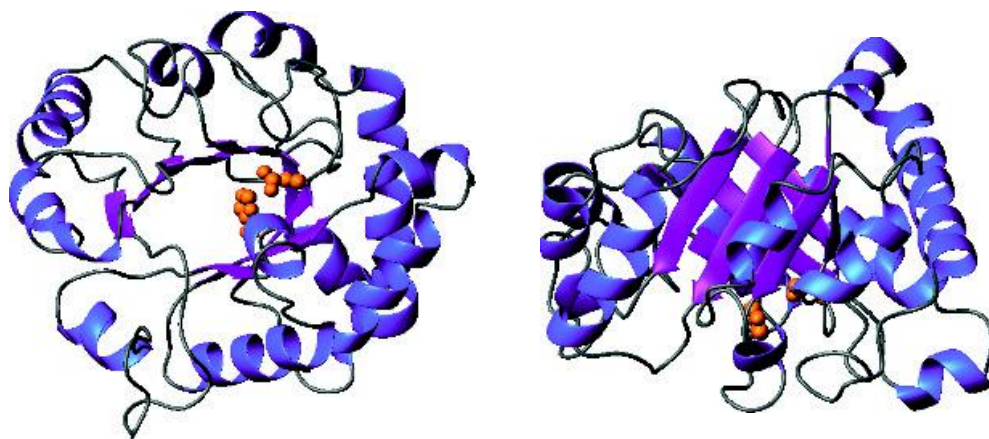


**Figure 7.36** Structure of triose phosphate isomerase monomer together with the active site residues surrounding substrate. Strands of the  $\beta$  barrel are shown in purple, helices in blue. The two critical residues of His95 and Glu165 are shown as solid spheres. The enzyme is shown from two orientations

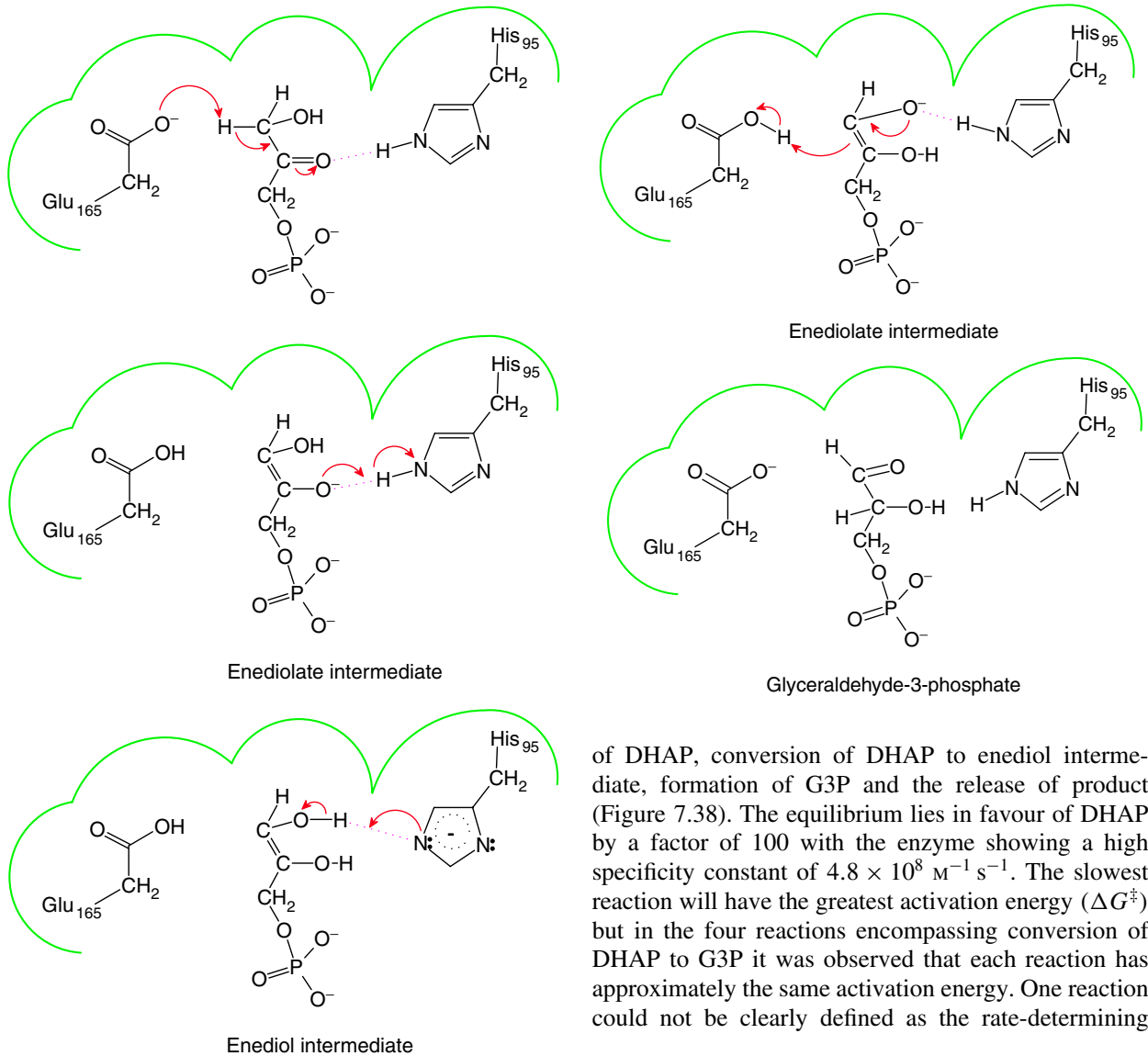


**Figure 7.37** The mechanism for conversion of DHAP to G3P in reactions catalysed by triose phosphate isomerase. The enzyme employs general acid–base catalysis with the uncharged histidine side chain acting as a proton donor whilst the charged imidazolite state acts as an acceptor. Alternative mechanisms have been proposed for this reaction including the removal of a proton from the OH group attached to the C1 and donation to the C2 oxygen by Glu<sub>165</sub>

of DHAP, conversion of DHAP to enediol intermediate, formation of G3P and the release of product (Figure 7.38). The equilibrium lies in favour of DHAP by a factor of 100 with the enzyme showing a high specificity constant of  $4.8 \times 10^8 \text{ M}^{-1} \text{ s}^{-1}$ . The slowest reaction will have the greatest activation energy ( $\Delta G^\ddagger$ ) but in the four reactions encompassing conversion of DHAP to G3P it was observed that each reaction has approximately the same activation energy. One reaction could not be clearly defined as the rate-determining

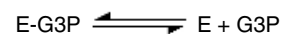
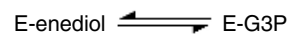
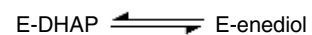
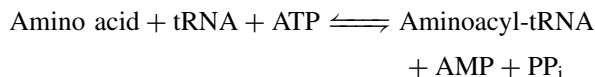


**Figure 7.38** The reactions of triose phosphate isomerase in a minimal kinetic scheme

step. This is unlikely to have arisen by accident and reflects catalytic ‘fine tuning’ to allow maximal efficiency. A  $k_{\text{cat}}$  of  $4 \times 10^3 \text{ s}^{-1}$  is not very high but the superb enzyme efficiency arises from a combination of fast turnover, effective tight binding of substrate ( $K_{\text{m}} \sim 10 \text{ }\mu\text{M}$ ) and transition state stabilization.

## Tyrosyl tRNA synthetase

The attachment of amino acid residues to tRNA molecules is a major part of the overall reaction of protein synthesis. The reaction involves the addition of activated amino acids by a group of enzymes known as amino acyl tRNA synthetases, and is summarized as



Any error at this stage is disastrous to protein synthesis and would lead to incorrect amino acid incorporation into a growing polypeptide chain. The error rate for most tRNA synthetases is extremely low and part of this efficiency comes from high discrimination during binding. Tyrosyl tRNA always binds tyrosine but never the structurally similar phenylalanine and the binding constant for tyrosine of  $2 \times 10^{-6} \text{ M}$  is at least five orders of magnitude smaller than that of phenylalanine.

Amino acids attach to tRNA molecules at the acceptor arm containing a conserved base sequence of -CCA-3'. Tyrosyl tRNA synthetase represents one of the simplest catalytic mechanisms known in biology with all activity deriving from binding interactions at the active site. The three-dimensional structure of tyrosyl tRNA synthetase from the *Bacillus stearothermophilus* is a dimer of subunits each containing 418 residues. (A dimer is an exception for most Class I tRNA synthetases which are generally monomeric, see Chapter 8.) The structure of the protein (Figure 7.39) has been determined with tyrosine and tyrosine-adenylate and is predominantly  $\alpha$  helical with a central six-stranded  $\beta$  sheet forming the core of the enzyme. The enzyme contains the Rossmann fold with tyrosyl adenylate bound at the bottom of the sheet with the phosphate groups reaching the surface of the protein. Although functionally a dimer the structure shown

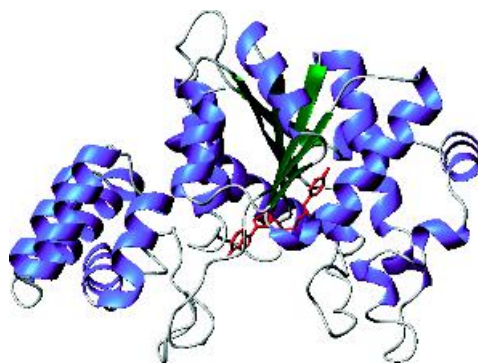


**Figure 7.39** The structure of tyrosyl tRNA from *B. stearothermophilus* in a complex with tyrosyl adenylate (PDB: 3TSI). Helices are shown in blue and the six stranded sheet in green. The bound tyrosyl adenylate is shown in red, with the adenylate portion situated on the left and the tyrosine pointing away from the viewer

is that of the monomer and represents the first 320 residues of the protein with remaining 99 residues at the C terminal found disordered. The monomer contains 220 residues in an amino terminal domain with  $\alpha/\beta$  structure together with a helix rich domain extending from residues 248–318 (shown on left of Figure 7.39).

The reaction catalysed by tyrosyl tRNA synthetase is divided into the formation of tyrosine adenylate (Tyr-AMP) and pyrophosphate from the initial reactants of tyrosine and ATP and then in a second reaction the Tyr-AMP is transferred to a specific tRNA. The structures of the enzyme bound with tyrosine, ATP and the tyrosyl adenylate intermediate are known and interactions between polypeptide chain and substrates or activated intermediate have been identified. These structures allowed individual residues to be identified as important for the formation of tyrosyl-adenylate – an intermediate stabilized by the enzyme and seen in crystal complexes.

Binding of substrate to tyrosyl tRNA synthetase is a random kinetic process with either tyrosine or ATP bound first. However, an examination of binding constants for each substrate suggests that ATP binding is weaker leading to an ordered process in which tyrosine binds first followed by ATP (Figure 7.40).

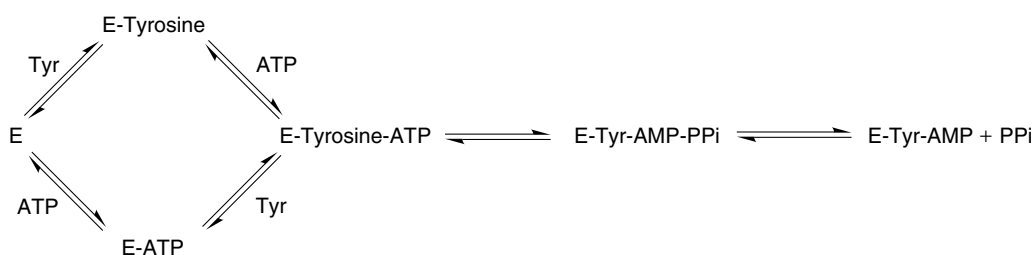


**Figure 7.40** Kinetic schemes for the formation of tyrosyl adenylate from tyrosine and ATP. This reaction represents the first part of the tyrosyl tRNA synthetase catalysed process. The products of the first reaction are tyrosyl adenylate (enzyme bound) and pyrophosphate (dissociates from ternary complex)

From the crystal structures in the presence of tyrosine and ATP it is apparent that residues Asp78, Tyr169 and Glu173 form a binding site for the  $\alpha$ -amino group of the tyrosine substrate. Not unexpectedly, the side chain of tyrosine forms hydrogen bonds via the phenolate group with residues Tyr34 and Asp176. The crystal structure of the complex with tyrosyl adenylate indicated that Cys35, Thr51 and His48 interact with the ribose ring (Figure 7.41).

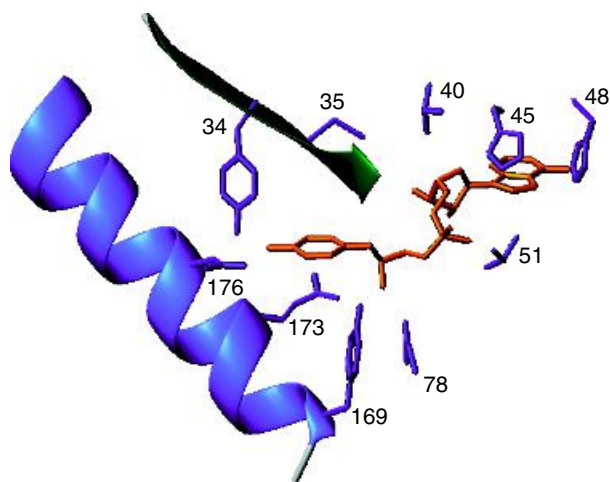


**Figure 7.41** Tyrosyl-adenylate binding to tyrosyl tRNA synthetase (PDB: 3TSI). Shown in orange is Tyr-AMP together with the side chains of Tyr34, Cys35, Thr40, His45, His48, Thr51, Asp78, Tyr169, Glu173 and Asp176

The role of residues in substrate binding was defined using mutagenesis to perturb the overall efficiency of tyrosyl tRNA synthetase. Cys35 was the first mutated residue and although in contact with the ribose ring of ATP and having a role in substrate binding it is remote from the critical active site chemistry based around the phosphate groups. Mutation of Cys35 to Gly estimated the effect of deleting the side chain hydrogen bonding interaction and revealed an enzyme operating with a lower efficiency by  $\sim 6 \text{ kJ mol}^{-1}$ . Modifying Tyr34 to Phe34 decreased the affinity of the enzyme for tyrosine, lowered the stability of the Tyr-AMP enzyme complex and decreased the ability of the enzyme to discriminate between tyrosine and phenylalanine. Mutagenesis combined with kinetic studies showed that changing Thr40 and His45 produced dramatic decreases in rates of Tyr-AMP formation. Changing Thr40 to Ala decreased Tyr-AMP formation by approximately 7000 fold whilst the mutation His45 to Gly caused a 200-fold decrease. A double mutant, bearing both substitutions, showed a decrease of  $\sim 10^5$ . In each case the affinity of the enzyme for substrate was unaltered but the affinity of the enzyme for the intermediate (Tyr-AMP..PP<sub>i</sub>) was lowered suggesting that Thr40 and His45 played key roles in stabilizing the transition state complex via interactions with inorganic pyrophosphate groups.

The single most important property of tRNA synthetases is substrate binding in pockets in restrained and extended conformation. The geometry lowers the activation energy barrier for the reaction and allows formation of the amino acyl adenylate complex. Two characteristic motifs with sequences His-Ile-Gly-His (HIGH) and Met-Ser-Lys (MSK) are important to

formation of the transition state. The close approach of negatively charged carboxyl groups (from the amino acid substrate) and the  $\alpha$  phosphate group of the ATP promotes formation of a transition state. The  $\alpha$  phosphate group is stabilized by interaction with His43 and Lys270 of the HIGH and MSK motifs. The pyrophosphate acts as a leaving group and the amino acyl adenylate transition state complex is stabilized by interactions with specific residues, as described in the preceding section.

The second half of the reaction, the transfer of the amino acid to the correct tRNA, has been examined through crystallization of other class I and class II tRNA synthetases (Table 7.6) with tRNA bound in a tight complex. The acceptor arm of tRNA and in particular the  $C_{74}C_{75}A_{76}$  base sequence binds alongside ATP in the active site. The arrangement of substrate in the active site of glutamyl tRNA synthetase (Figure 7.42) has been derived by using glutamyl-adenylate analogues (Figure 7.43) that co-crystallize with the enzyme defining interactions between residues involved in tRNA and amino acyl binding (Figure 7.44).

Gln tRNA synthetase must avoid selecting either glutamate or asparagine – two closely related amino acids. Discrimination between amino acids is favoured by recognition of both hydrogen atoms of the nitrogen in the glutamine side chain. Interactions involve the hydroxyl group of Tyr211 and a water molecule as obligatory hydrogen-bond acceptors in a network of

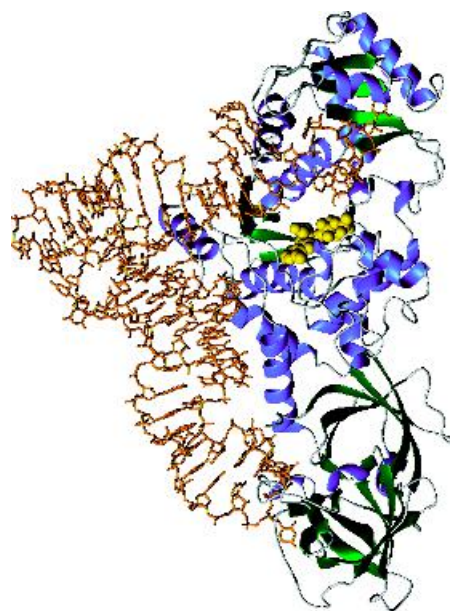


**Figure 7.42** Gln-tRNA synthetase showing complex of tRNA and ATP (PDB: 1GTG). The tRNA molecule is shown in orange with ATP in yellow. The secondary structure elements of enzyme are shown in blue (helices), green (strands) and grey (turns)

side chains and water molecules. In molecular recognition discrimination against glutamate and glutamic acid occurs because they lack one or both hydrogen atoms whilst the side chain of asparagine is too short.

**Table 7.6** Principal features of class I and class II aminoacyl tRNA synthetases

Property	Class I	Class II
Conserved substrate binding motifs	HIGH KMSKS	Motif 2 (FRxE) Motif 3 (GxGxGXER)
Dimerization motifs	None	Motif 1 (little consensus)
Active site fold	Parallel $\beta$ sheet of Rossmann fold	Antiparallel $\beta$ sheet
ATP conformation	Extended	Bent
Amino acylation site	2' OH	3'OH
tRNA binding	Variable loop faces solvent Binds to minor groove of acceptor stem	Variable loop faces protein Binds to major groove of acceptor stem



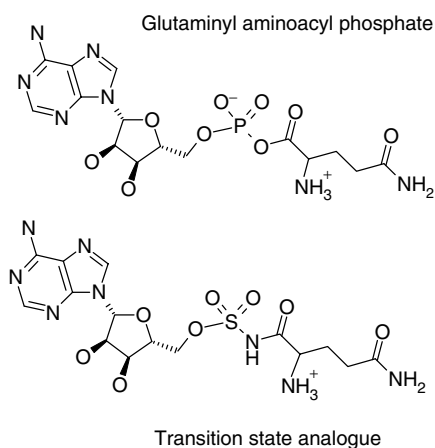


**Figure 7.43** Glutamyl amino acyl-adenylate and its transition state analogue

### EcoRI restriction endonuclease

Restriction enzymes were characterized through the 1960s and early 1970s, largely through the efforts of Werner Arber, Hamilton O. Smith and Daniel Nathans. The discovery of type II restriction endonucleases

represented a key event at the beginning of a new chapter of modern biochemistry. Subsequently, the use of type II restriction enzymes would allow manipulation of DNA molecules to create new sequences that would form the basis of molecular biology.

In addition to type II restriction endonucleases there are also type I and type III enzymes. Type I restriction enzymes have a combined restriction/methylation function within the same protein and cleave DNA randomly often at regions remote from recognition sites and often into a large number of fragments. They are not used in molecular cloning protocols. Type III restriction enzymes have a combined restriction/methylation function within the same protein but bind to DNA and at specific recognition sites. Again this class of enzymes is not routinely used in cloning procedures. In type II enzymes the restriction function is not accompanied by a methylase activity. Type II enzymes do not require ATP for activity although all enzymes appear to require Mg<sup>2+</sup> ions.

Currently more than 3000 type II restriction endonucleases have been discovered with more than 200 different substrate specificities. These enzymes are widely used in 'tailoring' DNA for molecular cloning applications. The substrate is double stranded DNA

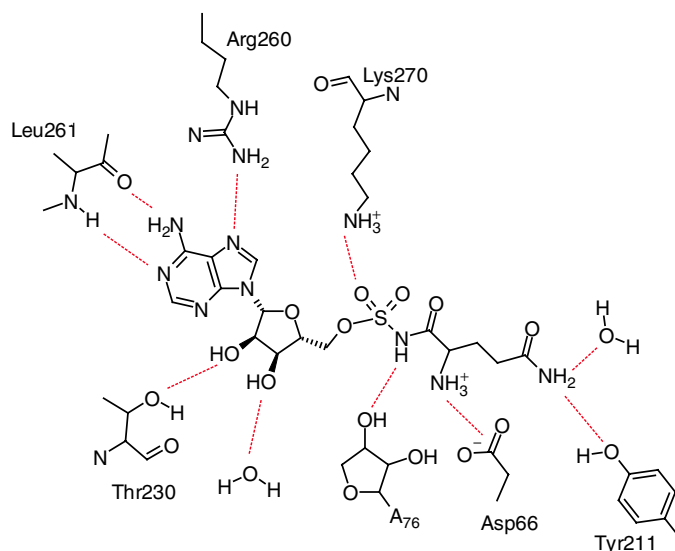


**Figure 7.44** The interaction between glutamyl adenylate analogue and the active site pocket of Gln-tRNA synthetase

**Table 7.7** A selection of restriction endonucleases showing cleavage sequences and sources. The arrows between bases indicate the site of cleavage within palindromic sequences

Enzyme	Recognition site	Source
AvaI	C↓(T/C)GG (A/G)G	<i>Anabaena variabilis</i>
BamHI	G↓GATCC	<i>Bacillus amyloliquefaciens</i> H
EcoRI	G↓AATTC	<i>Escherichia coli</i> RY13
HindIII	A↓AGCTT	<i>Haemophilus influenzae</i> Rd
NcoI	C↓CATGG	<i>Nocardia corallina</i>
PvuI	CGAT↓CG	<i>Proteus vulgaris</i>
SmaI	CCC↓GGG	<i>Serratia marcescens</i>
XhoI	C↓TCGAG	<i>Xanthomonas holcicola</i>

and in the majority of cases restriction endonucleases recognize short DNA sequences between 4 and 8 base pairs in length although in some instances longer sequences are identified. The names of restriction enzymes derive from the genus, species and strain designations of host bacteria (Table 7.7). So for example *EcoRI* is produced by *E. coli* strain RY13 whilst *NcoI* is obtained from *Nocardia corallina* and *HindIII* from *Haemophilus influenzae*.

Restriction enzymes recognize a symmetrical sequence of DNA where the top strand is the same as the bottom strand read backwards (palindromic). When *EcoRI* cuts the motif GAATTC it leaves overhanging chains termed ‘sticky ends’. The uncut regions of DNA remain base paired together. Sticky ends are an essential part of genetic engineering since they allow similarly cut fragments of DNA to be joined together.

*EcoRI* is one of the most widely used restriction enzymes in molecular biology and its structure has been determined by X-ray crystallography (Figure 7.45). The protein is a homodimer with each subunit containing a five-stranded  $\beta$  sheet flanked by helices. Subsequent determination of the structure

of other restriction enzymes such as *BamHI*, *BglII*, *Cfr10I*, *MunI*, and *NgoMIV* revealed significant fold similarity despite relatively low levels of sequence identity. This further suggested a common mechanism of catalytic action.<sup>1</sup> The *EcoRI* family share a substructure based around five  $\beta$  strands and two  $\alpha$  helices called the common core motif (CCM). The CCM is the result of a  $\beta$  meander followed by a binding pocket that interacts with recognition site DNA and is formed predominantly by two helices called the outer and inner helices. The core is readily seen by comparing structures of *EcoRI* complexed with DNA and devoid of its recognition partner.

The above view is, however, slightly misleading since whilst it portrays the secondary structure elements of the CCM it does not accurately reflect the action of the homodimer of subunits in surrounding DNA. The subunits bind to specific bases (GAATTC) in the major groove of the DNA helix with the minor groove exposed to the solvent. The dimers form a

<sup>1</sup>The other major structural family of restriction endonucleases is based around the structure of *EcoRV*.

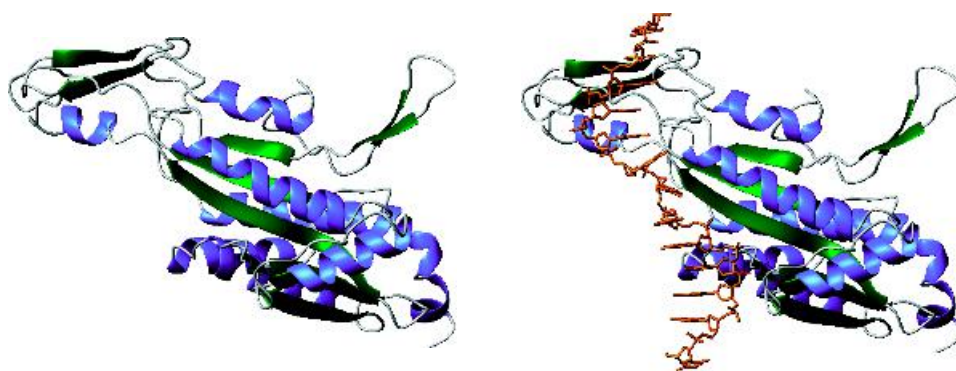


**Figure 7.45** The structure of *EcoRI* is shown with and without a recognition sequence of DNA. The five-stranded  $\beta$  sheet making up most of the CCM is shown in the centre of the protein in green

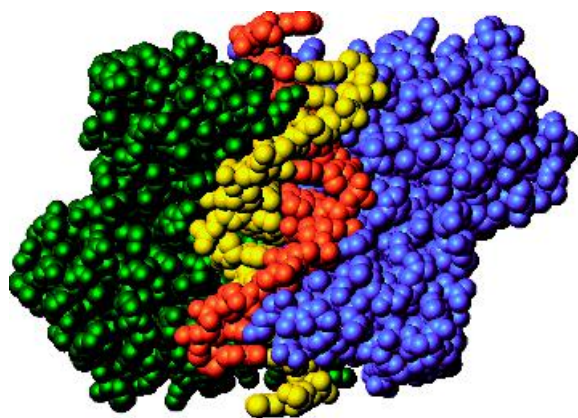


**Figure 7.46** Space filling representation of homodimer of *EcoRI* bound to DNA. The subunits of the enzyme are shown in blue and green whilst the DNA is shown in orange/yellow. The minor groove is exposed to the solvent

cleft lined with basic residues that associate with sugar-phosphate chains via charge interactions (Figure 7.46). Of more importance are arginine side chains at residues 145 and 200, together with a glutamate side chain (Glu144) in each monomer that form hydrogen bonds with base pairs of the recognition motif. This confers specificity to the binding reaction with DNA and avoids interactions with incorrect, but often closely related, sequences. Sequence specificity is mediated by 16 hydrogen bonds originating from  $\alpha$  helical

recognition regions. Twelve of the hydrogen bonds occur between protein and purine whilst four exist between protein and pyrimidine. *EcoRI* ‘reads’ all six bases making up the recognition sequence by forming interactions with each of them. Arg200 forms two hydrogen bonds with guanine while Glu144 and Arg145 form four hydrogen bonds to adjacent adenine residues. In addition to the hydrogen bonds an elaborate network of van der Waals contacts exist between bases and recognition helices. It is these interactions that discriminate the *EcoRI* hexanucleotide GAATTC from all other hexanucleotide sequences. Changes in base identity lose hydrogen bonds and effectively discriminate between different sequences. Hydrogen bond formation distorts the DNA helix introducing strain and a torsional kink in the middle of its recognition sequence leading to local DNA unwinding. The unwinding involves movement of DNA by  $\sim 28^\circ$  and groove widening by  $\sim 0.35$  nm where ‘strain’ may enhance catalytic rates.

The presence of divalent cations ( $\text{Mn}^{2+}$ ,  $\text{Co}^{2+}$ ,  $\text{Zn}^{2+}$  and  $\text{Cd}^{2+}$ ) results in bond scission but in their absence enzymes shows low activity. The use of electron dense ions pinpoints the metal centre location as close to Glu111 in co-crystals of protein–DNA–divalent ion and emphasizes the role of a metal centre in catalysis. Metal ions are coordinated in the vicinity of the active site acidic side chains. The observation of mono and binuclear metal centres within active sites of restriction endonucleases suggests that

although the structure of the active site-DNA binding region of many enzymes is similar the catalytic mechanisms employed may differ from one enzyme to another.

Restriction endonucleases contain a signature sequence D-(X)<sub>n</sub>-D/E-Z-K, in which three residues are *weakly* conserved (D, D/E and K). The two acidic residues are usually Asp, although Glu occurs in *EcoRI* and several other restriction endonucleases, including *BamHI*. These residues are separated by 9–20 residues and are followed by a basic lysine side chain preceded by Z, a residue with a hydrophobic side chain. In *EcoRI* the catalytic residues are Asp91, Glu111 and Lys113, whilst Asp59, preceding the conserved cluster, also appears to be important to catalysis. These residues make up the active site, whilst in *BamHI* the corresponding residues are Asp94, Glu111, and Glu113 with Glu77 preceding the cluster of charged residues. *BamHI* cuts the sequence GGATTC – a hexanucleotide sequence almost identical to that recognized by *EcoRI* (GAATTC) – yet each enzyme shows absolute specificity for its own sequence. Both enzymes possess homodimeric structures with a catalytic core region of ~200–250 residues per monomer consisting of five strands and two helices. However, the method of sequence recognition and potential mechanism of catalysis in two clearly related enzymes appears to differ. The catalytic mechanism for *EcoRI* involves a single metal ion whilst that of *BamHI* involves two cations (Figure 7.47). Similarly, DNA

binding through base contacts in the major groove uses a set of loops between strands together with  $\beta$  strands (*EcoRI*) whilst *BamHI* lacks these regions and uses the N-terminal end of a helix bundle. Despite a lack of agreement conclusions can be drawn about the requirements for phosphodiester bond cleavage in any restriction enzyme. At least three components are required; a general base is needed to activate water, a Lewis acid is necessary to stabilize negative charge formed in the transition state complex and a general acid is required to protonate the leaving group oxygen.

## Enzyme inhibition and regulation

Enzymes are inhibited and regulated. Studying each process sheds light on the control of catalysis, catalytic pathways, substrate binding and specificity, as well as the role of specific functional groups in active site chemistry. Inhibition and regulation are inter-related with cells possessing proteins that inhibit enzymes as part of a normal cellular function.

Reversible inhibition involves non-covalent binding of inhibitor to enzyme. This mode of inhibition is shown by serpins, proteins that act as natural trypsin inhibitors preventing protease activity. The complex formed between bovine pancreatic trypsin inhibitor (BPTI) and trypsin has extraordinary affinity with a large association constant ( $K_a$ ) of  $\sim 10^{13} \text{ M}^{-1}$ . Tight association between proteins causes effective enzyme

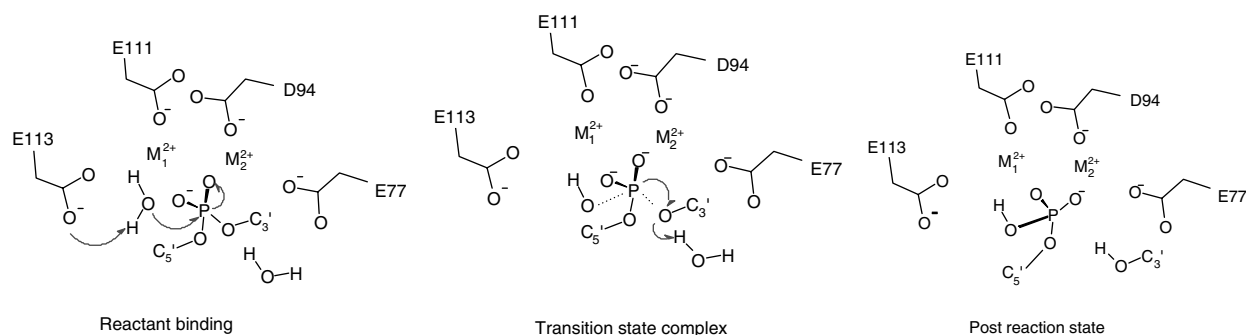


**Figure 7.47** A general mechanism of catalysis for type II restriction endonucleases based on *BamHI*. The reaction occurs through an  $S_N2$  mechanism, with an in-line displacement of the 3'-OH group and an inversion of configuration of the 5'-phosphate group

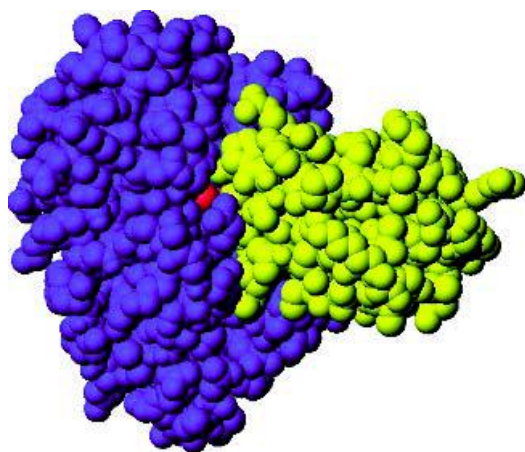


**Figure 7.48** Binary complex formed between trypsin and BPTI showing insertion of Lys15 (red) into the specificity pocket. Trypsin is shown in blue, BPTI in yellow (PDB: 2PTC)

inhibition and crystallography of the protein complex reveals a tightly packed interface between BPTI and trypsin formed by numerous intermolecular hydrogen bonds (Figure 7.48). On the surface of BPTI Lys15 occupies the specificity pocket of trypsin with a Lys–Ala peptide bond representing the scissile region. However, bond cleavage does not occur despite the proximity of Ser195 and the formation of a tetrahedral intermediate. Absence of bond cleavage results from tight binding between BPTI and enzyme that prevents diffusion of the leaving group (peptide) away from the active site and restricts access of water to this region.

By measuring reaction kinetics at different conditions activity profiles ( $k_{\text{cat}}/K_{\text{m}}$ ) are determined for individual enzymes. Extremes of pH lead to a loss of activity as a result of enzyme denaturation and solutions of pH 2.0 do not in general support folded structure and lead to a loss of activity that is restored when the pH returns to normal values. Reversibility is observed because covalent modification of the enzyme does not occur.

Investigating kinetic profiles for enzyme-catalysed reactions in the presence of an inhibitor may identify mechanisms of inhibition and provides important clues

in the absence of structural data of the active site geometry and composition. Armed with structural knowledge the pharmaceutical industry has produced new inhibitors with improved binding or inhibitory action that play crucial roles in the battle against disease. The starting point for enzyme inhibitor studies is often identification of a natural inhibitor. When inhibitor data is available with detailed structural knowledge of an enzyme's active site it becomes possible to enter the area of rational drug design. This combines structural and kinetic data to design new improved compounds and is often performed on computers. With a family of 'lead in' compounds chemical synthesis of a restricted number of favourable targets, followed by assays of binding and inhibition, can save years of experimental trials and allows drugs to enter clinical trials and reach the marketplace. Such approaches combining classical enzymology with bioinformatics and molecular modelling allows development of new pharmaceutical arsenals and a new approach to molecular medicine. Using these techniques enzyme inhibitors have been introduced to counteract emphysema, HIV infection, alcohol abuse, inflammation and arthritis.

The most important type of reversible inhibition is that caused by molecules that compete for the active sites of enzymes (Figure 7.49). The competitor is almost always structurally related to the natural substrate and can combine with the enzyme to form an enzyme–inhibitor complex analogous to that formed between the enzyme and the substrate. Occasionally the 'inhibitor' is converted into product but more frequently inhibitors bind to active sites without undergoing further catalytic reactions.

When the enzyme binds inhibitor it is unable to catalyse reactions leading to products and this is observed by a decrease in enzyme activity at a given substrate concentration. A usual presentation of competitive inhibition involves Eadie–Hofstee or Lineweaver–Burk plots, and is marked by a decrease in  $K_{\text{m}}$  although the overall  $V_{\text{max}}$  remains similar between inhibited and uninhibited reactions (Figures 7.50 and 7.51).  $V_{\text{max}}$  is unchanged because addition of substrate in high concentrations will effectively displace inhibitor from the active site of an enzyme leading to unimpeded rates of reaction.

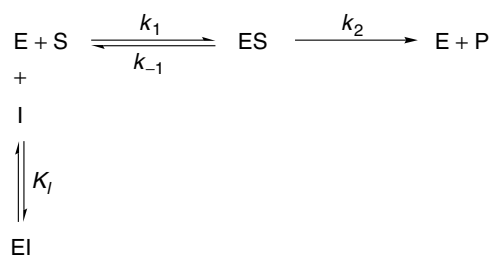


**Figure 7.49** Competitive inhibition leads to additional reactions in Michaelis–Menten schemes

The rate equations are solved exactly as before, except that the total enzyme concentration is equivalent to

$$[\text{E}]_{\text{T}} = [\text{E}] + [\text{ES}] + [\text{EI}] \quad (7.48)$$

and leads to an expression for the initial velocity  $v$

$$v = k_{\text{cat}}[\text{E}]_{\text{T}}[\text{S}] / K_{\text{m}}(1 + [\text{I}]/K_{\text{I}}) + [\text{S}] \quad (7.49)$$

The  $K_{\text{m}}$  is increased by a factor of  $(1 + [\text{I}]/K_{\text{I}})$  with the second ‘apparent’  $K_{\text{m}}$  shown in the following equation as  $K_{\text{APP}}$

$$v = V_{\text{max}}[\text{S}] / K_{\text{APP}} + [\text{S}] \quad (7.50)$$

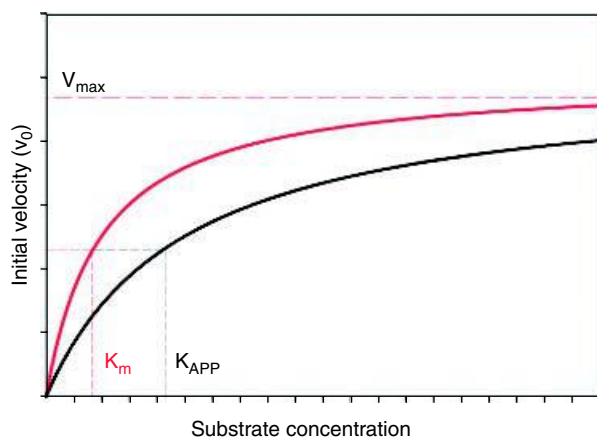


**Figure 7.50** An enzyme-catalysed reaction showing a plot of initial velocity against substrate concentration in the presence (black trace) and absence (red trace) of inhibitor

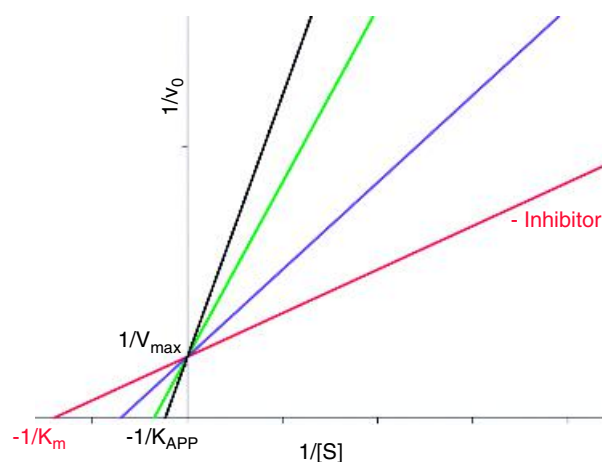


**Figure 7.51** Lineweaver–Burk plot of an enzyme-catalysed reaction with competitive inhibition. With  $K_{\text{APP}}$  determined at several different inhibitor concentrations a plot of  $K_{\text{APP}}$  versus  $I$  will yield a straight line whose gradient is  $K_{\text{m}}/K_{\text{I}}$ , where  $K_{\text{m}}$  can be estimated from the line’s intercept where  $[I] = 0$ . Alternatively  $K_{\text{m}}$  can be estimated from the Lineweaver–Burk plot

One example of competitive inhibition is seen in succinate dehydrogenase and the conversion of succinate to fumarate as part of the citric acid cycle. Malonate is a competitive inhibitor of succinate dehydrogenase and with structural similarity to succinate, binds at the active site but does not undergo dehydrogenation (Figure 7.52). The observation of competitive inhibition suggests binding involves the two carboxylate groups. A further example of competitive inhibition is benzamidine, a structural analogue of arginine, that binds to the active site of trypsin (Figure 7.53).

The remaining patterns of reversible inhibition are called uncompetitive and non-competitive (or mixed) inhibition. Uncompetitive inhibition involves binding directly to enzyme–substrate complexes but not to free enzyme (Figure 7.54). As such there is no requirement for an uncompetitive inhibitor to resemble the natural substrate and it is generally believed that inhibition arises from a distortion of the active site region preventing further turnover.

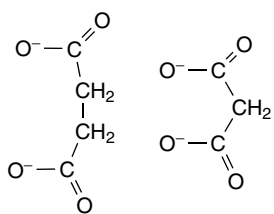


**Figure 7.52** The structures of succinate and malonate

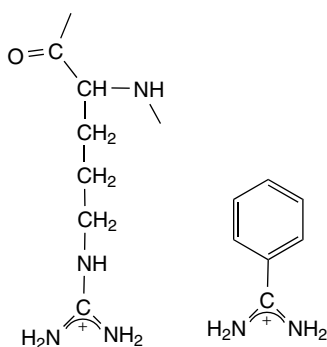


**Figure 7.53** Benzamidine and arginine. Competitive inhibitor and substrate in trypsin

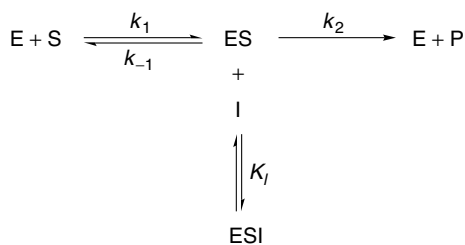


**Figure 7.54** Kinetic scheme illustrating uncompetitive inhibition of enzyme-catalysed reaction

Non-competitive inhibition (Figure 7.55) involves inhibitor binding to free enzyme and enzyme substrate complexes to form inactive EI or ESI states. It is comparatively rare but is exhibited by some allosteric enzymes. In these cases it is thought that inhibitor binds to the enzyme causing a change in conformation that permits substrate binding but prevents further catalysis.

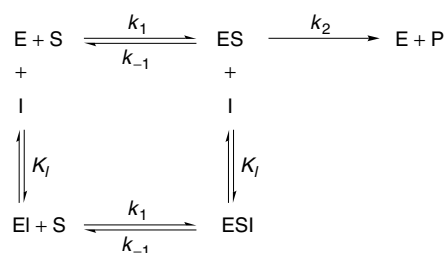


**Figure 7.55** Kinetic scheme describing non-competitive inhibition. In the above example numerous kinetic simplifications have been introduced. The complex ESI can sometimes exhibit catalytic activity at reduced rates, or the binding of inhibitor may alter substrate binding and/or  $k_{cat}$ . As a result of these differential effects the term mixed inhibition is used

Since a non-competitive inhibitor binds to both E and ES removing catalytic competence in the latter the effect of this is to lower the number of effective enzyme molecules. The result is a decrease in  $V_{max}$  as a result of changes in  $k_{cat}$ . Since non-competitive inhibitors bind at sites distinct from the substrate there is not normally any effect on  $K_m$ .

## Irreversible inhibition of enzyme activity

Irreversible inhibition can involve the inactivation of enzymes by extremes of pH, temperature or chemical reagents. Most frequently, however, it involves the covalent modification of the enzyme in a manner that destroys activity. Most substances that cause irreversible inhibition are toxic to cells, although in the case of aspirin the 'toxic' effect is beneficial. Many irreversible inhibitors have been identified; some are naturally occurring metabolites whilst others result from laboratory synthesis (Table 7.8).

The inhibition of enzymes involved in bacterial cell wall synthesis is exploited through the use of penicillin as an antibiotic that binds to bacterial enzymes involved in cell wall synthesis causing inactivation. The inability to extend bacterial cell walls prevents division and leads to the cessation of bacterial growth and limits the spread of the infection.

**Table 7.8** Irreversible enzyme inhibitors and sites of action

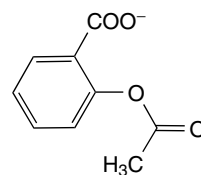
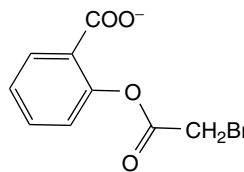
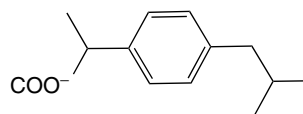
Compound	Common source and site of action
Diisopropylfluorophosphate (DIFP), Sarin	Synthetic; inactivate serine residues of serine protease enzymes
Ricin/abrin	Castor bean; ribosomal inactivating proteins; inhibit ribosome function via depurination reactions
<i>N</i> -tosyl-L-phenylalanine chloromethylketone (TPCK)	Synthetic inhibitor; binds to active site histidine in chymotrypsin
Penicillin	Naturally occurring antibiotic plus many synthetic variants; inhibits cell wall biosynthesis enzymes particularly in Gram-positive bacteria
Cyanide	Released during breakdown of cyanogenic glycosides found in many plants; inhibits respiration
Aspirin	Natural product – methyl salicylate plus synthetic variants. All bind to active site of cyclo-oxygenase inhibiting substrate binding

### *Aspirin: an inhibitor of cyclo-oxygenases*

Aspirin's pain-killing capacity was known to Hippocrates in the 5th century BC but provides a marvelous example of how studies of enzyme inhibition combined with structural analysis leads to advances in health care.

Prostaglandins are hormones created by cells that act only in the local or surrounding area before they are broken down. Unlike most hormones they are not transported systemically around the body but control 'local' cellular processes such as the constriction of blood vessels, platelet aggregation during blood clotting, uterine constriction during labour, pain transmission and the induction of inflammation. Although these diverse processes are controlled by different prostaglandins they are all created from a common precursor molecule called arachidonic acid. Cyclo-oxygenase catalyses the addition of two oxygen molecules to arachidonic acid in a pathway that leads to the formation of prostaglandins.

Aspirin-like drugs, sometimes called non-steroidal anti-inflammatory drugs or NSAIDs (Figure 7.56), prevent prostaglandin biosynthesis through inhibition of cyclo-oxygenases such as COX-1 (Figure 7.57).

**Aspirin****Bromoaspirin****Ibuprofen**

**Figure 7.56** Three common non-steroidal anti-inflammatory drugs (NSAIDs)

Crystallization of cyclo-oxygenase by R. Garavito showed a membrane protein comprised of three



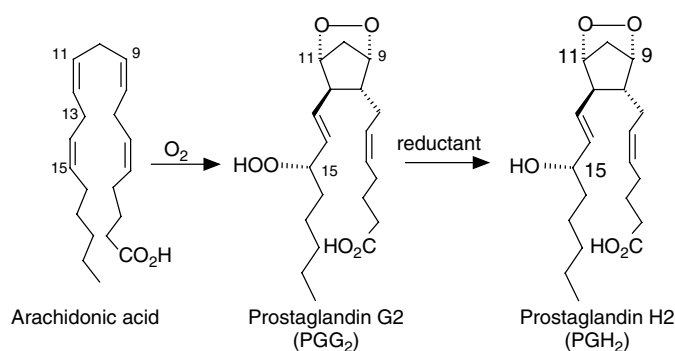


**Figure 7.57** Formation of prostaglandin H<sub>2</sub> from arachidonic acid by cyclo-oxygenase

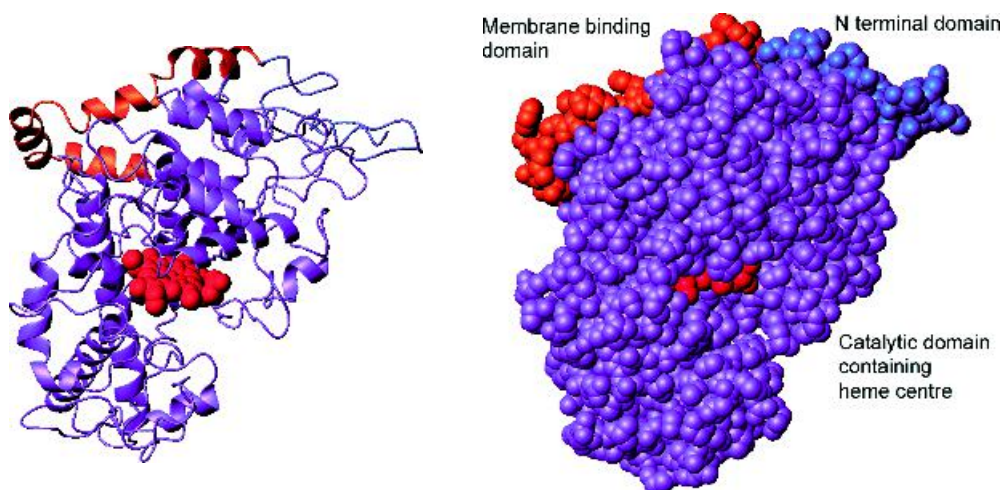


**Figure 7.58** The three-dimensional structure of cyclo-oxygenase (PDB:1PRH). On the left the distribution of secondary structure is shown for one subunit of the dimer found in the crystal lattice. The space filling model highlights the different domains and the buried heme group. (blue, residues 33–72; orange, membrane-binding region formed from residues 73–116; and purple the globular domain containing the catalytic heme group)

domains in a chain of 551 residues (Figure 7.58). Residues 33–72 form a small compact module whilst a second domain (residues 73–116) adopts a right-handed spiral of four helical segments along one side of the protein. This domain binds to the membrane via amphipathic helices. The third domain is the catalytic heart of the bifunctional enzyme performing cyclo-oxygenation and peroxidation. Cyclo-oxygenase is a homodimer, and should be more correctly called prostaglandin H synthase (or PGHS-1) because the

cyclo-oxygenase reaction is only the first of two functional reactivities.

The cyclo-oxygenase reaction occurs in a hydrophobic channel that extends from the membrane-binding domain to the catalytic core and a non-covalently bound heme centre. The arachidonic acid is positioned in this channel in an extended L-shaped conformation and catalysis begins with abstraction of the 13-pro-*S*-hydrogen to generate a substrate bound radical. At this point, a combination of active site residue interactions

and conformational changes control the regio- and stereospecific additions of molecular oxygen and ring closures resulting in the product.

Insight into the mechanism of action of aspirin stemmed from crystallization of this protein in the presence of inhibitors. In the bromoaspirin-inactivated structure Ser530 is bromoacetylated (as opposed to simple acetylation with aspirin) with the salicylate leaving-group bound in the tunnel as part of the active site (Figure 7.59). The bound salicylate group blocks substrate access to the heme centre whilst other NSAIDs do not covalently modify the enzyme but prevent conversion of arachidonic acid in the first reaction of prostaglandin synthesis. The active site is essentially a hydrophobic channel of highly conserved residues such as Arg120, Val349, Tyr348, Tyr355, Leu352, Phe381, Tyr385, and Ser530. At the mouth of the channel lie Arg120 and Tyr 355 and these residues interact with the carboxylate groups of arachidonic acid with the remainder of the eicosanoid chain extending into the channel and binding to hydrophobic residues close to Ser530. Although the details of catalysis and inhibition remain to be clarified the heme group lies at one end of the channel and it is thought

that heme-catalysed peroxidase activity involves the formation of a tyrosyl radical to initiate the process.

Aspirin is an extremely beneficial drug but concern exists over the damage caused to the stomach and duodenum in significant numbers of patients. About one in three people who take NSAIDs for long periods develop gastrointestinal bleeding. The underlying reasons for the unwanted side effects became clear with the realization that two forms of cyclo-oxygenase (COX-1 and COX-2) exist *in vivo*. COX-1 is the constitutive isoform whilst COX-2 is induced by inflammatory stimuli. The beneficial anti-inflammatory actions of NSAIDs are due to inhibition of COX-2 whereas unwanted side effects such as irritation of the stomach lining arise from inhibition of COX-1. It is clearly desirable to obtain enzyme inhibitors (drugs) that selectively target (inhibit) COX-2.

Despite different physiological roles COX-1 and COX-2 show similar structures and catalytic functions, with a small number of amino acid substitutions giving rise to subtle differences in ligand interaction between each isoform. These differences form the basis of developing structure–function relationships in cyclo-oxygenases and allow rational drug design aimed at improving the desirable properties of aspirin without

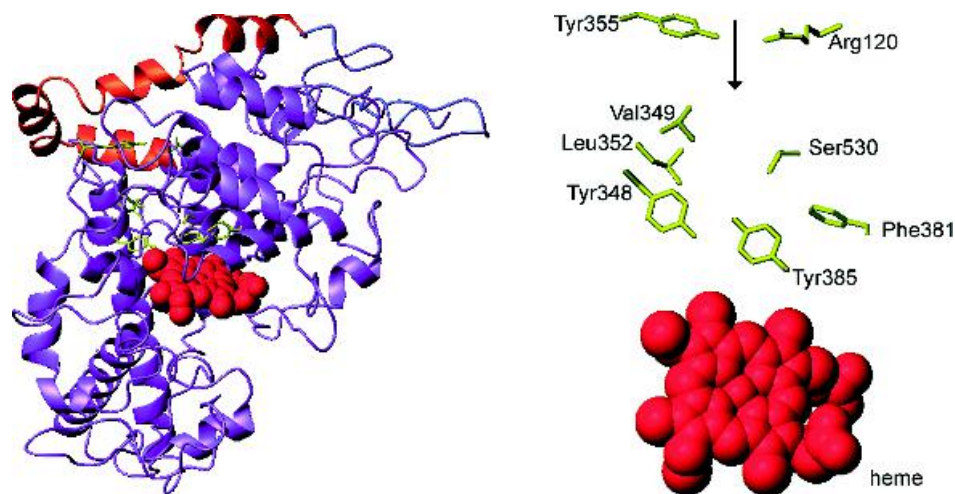


**Figure 7.59** The active site of cyclo-oxygenase (COX-1) shown by the yellow residues superimposed on the secondary structure elements. Removing the bulk of the protein shows the approximate position of the channel (arrow) and the lining of this pocket by conserved residues. Ser530, acetylated by aspirin, lies approximately midway along the channel

any of the unwanted side effects. As a result new and improved products are reaching the marketplace, with one product, Celebrex<sup>®</sup>, introduced in 1999 as a potent selective inhibitor of COX-2 designed to relieve pain associated with osteoarthritis and adult rheumatoid arthritis.

## Allosteric regulation

Although inhibition is one form of regulation it tends to be ‘all or nothing’ and the cell has of necessity devised better methods of control. The concept of regulation of protein activity by molecules known as effectors was demonstrated in haemoglobin. Binding to a site between individual subunits by 2,3 DPG caused conformational changes in haemoglobin that modulated oxygen affinity. The principle of regulation by molecules unrelated to substrate is the basis of allostery with studies on haemoglobin pioneering the development of this area.

Allosteric enzymes have at least two subunits (exhibit quaternary organization) with multiple catalytic and binding sites. In general the active and inactive forms undergo conformational changes arising from effector binding at sites distinct from the catalytic centres. Allosteric regulation is shown by large numbers of enzymes but particularly those involved in long metabolic pathways. These pathways include biosynthetic reactions, glycolysis, glycogenesis and  $\beta$  oxidation. Here, the effectors are often components of the metabolic pathway and their presence serves to inhibit or stimulate activity in a manner that allows exquisite control over a reaction pathway. Allosteric modulators bind non-covalently to the enzyme and can precipitate changes in either  $K_m$  for the substrate or  $V_{max}$  of the enzyme.

Allosteric enzymes are multimeric proteins, but can be composed of identical or non-identical subunits. Allosteric enzymes made up of identical subunits include phosphofructokinase (PFK) glycogen phosphorylase, and glycogen synthase. For enzymes composed of identical subunits each polypeptide chain contains at least one catalytic and one regulatory site whilst for enzymes composed of non-identical subunits these sites can be on different subunits, but this is not obligatory. Allosteric enzymes composed of non-identical subunits

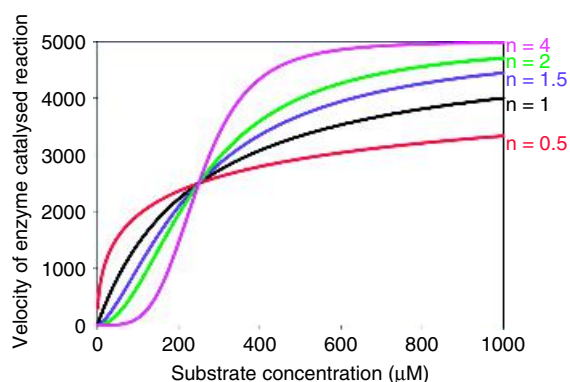


**Figure 7.60** A plot of  $v_0$  versus  $[S]$  for an allosteric enzyme. In the different curves the  $V_{max}$  and  $K_{0.5}$  are constant at 1000 and 250 whilst the Hill coefficient ranges from 0.5, 1, 1.5, 2, and 4, respectively

include aspartate transcarbamoylase, lactate dehydrogenase, pyruvate kinase, and protein kinase A.

Allosteric enzymes are identified from plots of initial velocity versus substrate concentration. For at least one substrate this profile will not exhibit the normal hyperbolic variation of  $v_0$  with  $[S]$  but shows a sigmoidal profile (Figure 7.60). This is an example of positive substrate cooperativity and a plot of  $v_0$  against  $[S]$  is defined by the Hill equation. The Hill equation is expressed as

$$v = V_{max}[S]^n / K_{0.5}^n + [S]^n \quad (7.53)$$

where  $K_{0.5}$  is the substrate concentration at half maximal velocity. Since this description is not the Michaelis–Menten equation it should not be called the  $K_m$ , although within the literature this term is frequently found. The parameter  $n$ , the Hill coefficient, can be greater or less than 1. A value of 1 gives hyperbolic profiles whilst other values yield curves showing cooperativity.

In PFK the profile of  $v$  against  $[S]$  with ATP as a substrate exhibits Michaelis–Menten kinetics but with fructose-6-phosphate the profile is sigmoidal (Figure 7.61). PFK is found universally in prokaryotes and eukaryotes as one enzyme in the pathway of glycolysis and catalyses the conversion of fructose 6-phosphate into fructose 1,6 diphosphate. In eukaryotic cells PFK activity is inhibited by ATP and citrate

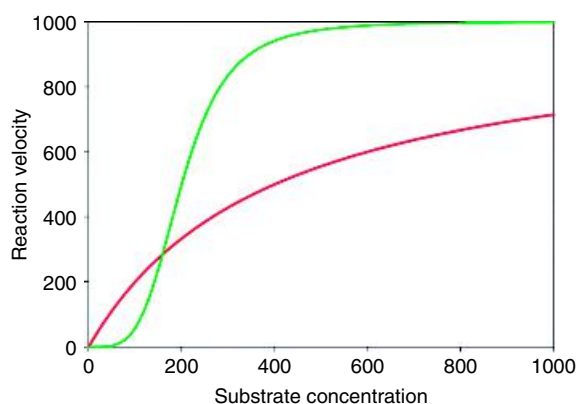


**Figure 7.61** The sigmoidal and hyperbolic kinetics for PFK in the presence of effector (fructose-6-phosphate) and normal substrate (ATP)  
 $\text{Fructose-6-phosphate} + \text{ATP} \rightleftharpoons \text{Fructose 1,6diphosphate} + \text{ADP}$

whilst activation occurs with ADP, AMP and cyclic AMP. In bacteria the PFK enzymes are structurally simpler with a diverse array of allosteric modulators. The most studied PFKs are isolated from *B. stearothermophilus* and *E. coli*. These enzymes are inhibited by

phosphoenolpyruvate (an end product of glycolysis) and stimulated by ADP as well as GDP.

PFK is a homotetramer containing polypeptide chains of 320 residues each folded into two domains. These domains are of different structure with domain 1 formed by residues 1–141 and residues 256–300 containing  $\alpha$  and  $\beta$  secondary structure ( $\alpha/\beta$ ) and domain 2 formed by residues 142–255 and the C-terminal sequence forming an  $\alpha$ - $\beta$ - $\alpha$  layered structure (Figure 7.62). Each subunit has 12  $\alpha$  helices and 11  $\beta$  strands and forms a large contact area with an identical subunit creating a dimer. Dimers associate through smaller interfacial contact zones forming the tetramer. Initial studies of the enzyme showed that one of the products of the reaction (ADP) together with  $\text{Mg}^{2+}$  ions bind to the larger domain (blue) whilst an allosteric regulator (ADP again) is also found attached to the smaller second domain (orange). In this instance the effector molecule (ADP) resembles the structure of one of the substrates (ATP) and represents an example of homotypic regulation (Figures 7.63 and 7.64).

The active site for ADP and fructose-6-phosphate binding is formed between two subunits in a cleft. The T state of PFK has a low affinity for fructose-6-phosphate (substrate) whilst the R form has a much higher affinity.

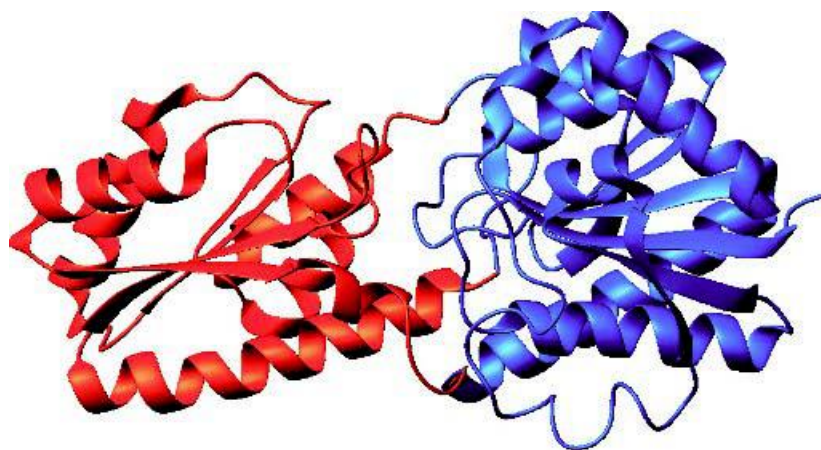


**Figure 7.62** The arrangement of domains 1 and 2 within a single subunit of PFK. Shown in blue is the domain encompassing residues 1–138 and 256–305 whilst in orange is the secondary structure of residues 139–255 and 306–319

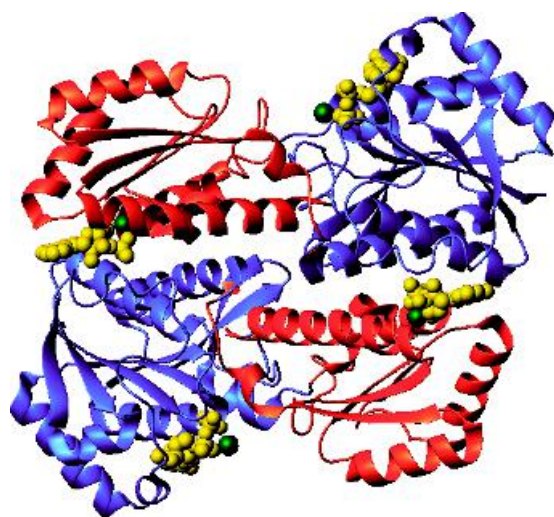


**Figure 7.63** The arrangement of domains 1 and 2 within the PFK dimer showing ADP and  $Mg^{2+}$  ions bound to the different parts of the enzyme. ADP is shown in yellow,  $Mg^{2+}$  ions in green with the large and small domains of each subunit shown using the colour scheme of Figure 7.62. The dimers associate forming the binding site for the effector ADP molecule

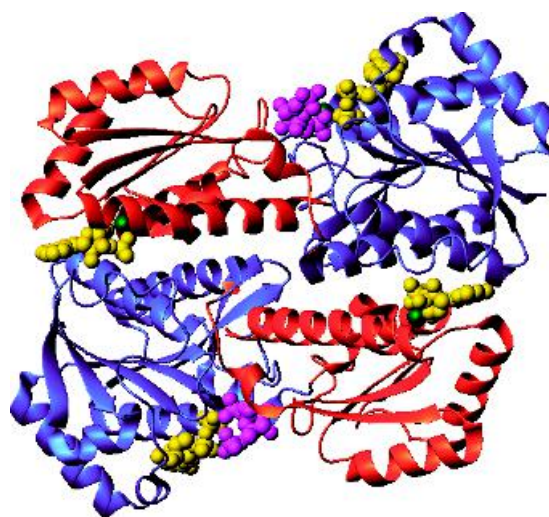


**Figure 7.64** The arrangement of domains 1 and 2 within a PFK dimer showing fructose-6-bisphosphate (magenta) and ADP/ $Mg^{2+}$  bound to the active site of the large domain. These are the products of the reaction and the structure is the R state enzyme. ADP/ $Mg^{2+}$  is also bound at the effector site located on the smaller domain (PDB:1PFK). Only the dimer is shown and it should be remembered an additional dimer of subunits is present in the PFK homotetramer

Alongside fructose-6-phosphate ATP is also bound at the active site whilst at the allosteric site ATP (inhibitor) and ADP (activator) bind in addition to phosphoenolpyruvate (PEP), a second allosteric inhibitor. The allosteric sites are located principally in the smaller effector domain (orange section in Figures 7.63 and 7.64) but form contacts with the active site domain of neighbouring dimers. As a result of this arrangement conformational changes occurring at allosteric sites are easily transmitted to the active site domains of other subunits.

An analogue of PEP, 2-phosphoglycolate, binds tightly to the allosteric site yielding an inhibited form of the enzyme equivalent to the T state. By comparing the structure of T state enzyme with that formed in the presence of products (R state) the extent of conformational changes occurring in PFK were estimated. The crystal structures of PFK determined in the R and T states suggest the structural differences reside in rotation of dimers relative to one another. Comparing the inhibited state with the active state

showed that the tetramer twists about its long axis so that one pair of subunits rotates relative to the other pair by about  $8^\circ$  around one of the molecular dyad axes. This rotation partly closes the binding site for the cooperative substrate fructose-6-phosphate and therefore explains its weaker binding to this conformational state. A single subunit contains two domains and the R > T transition also involves rotation of these regions relative to each other by  $\sim 4.5^\circ$  that further closes the active (fructose-6-phosphate) site between domains. Another consequence of these movements is to alter the orientation of residues lining the catalytic pocket. In the R state two arginine side chains form ionic interactions with fructose-6-phosphate whilst a glutamate side chain is displaced out of the pocket. In the T state movement of dimers results in Arg162 pointing away from the binding site and Glu161 facing into the binding site. The effect of replacing a positive charge with a negative charge at the active site is

to decrease fructose 6-phosphate binding by repulsion between negatively charged groups. PFK appears to represent a simple allosteric kinetic scheme in which the active and the inhibited conformations differ in their affinities for fructose-6-phosphate but do not differ in their catalytic competence. The presence of two conformational states is very similar to that previously described for haemoglobin.

Aspartyl transcarbamoylase (ATCase) is a large complex composed of 12 subunits of two different types. The enzyme catalyses formation of *N*-carbamoyl aspartate from aspartate and *N*-carbamoyl phosphate, and is an early step in a unique and critical biosynthetic pathway leading to the synthesis of pyrimidines (such as cytosine, uracil and thymine; Figure 7.65).

Both aspartate and carbamoyl phosphate bind cooperatively to the enzyme giving sigmoidal profiles (Figure 7.66) that are altered in the presence of cytidine triphosphate (CTP), a pyrimidine nucleotide, and adenosine triphosphate (ATP), a purine nucleotide. Allosteric inhibition is observed in the presence of CTP whilst ATP induces allosteric activation. Experimentally, a plot of  $v_0$  against  $[S]$  is observed to be sigmoidal and to shift to the left in the presence of ATP

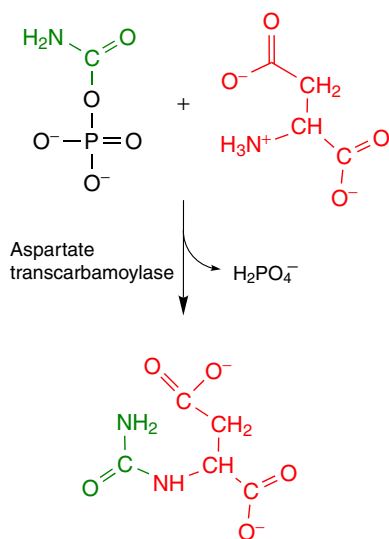


**Figure 7.65** Initial reaction of pyrimidine biosynthesis involving condensation of aspartate and carbamoyl phosphate

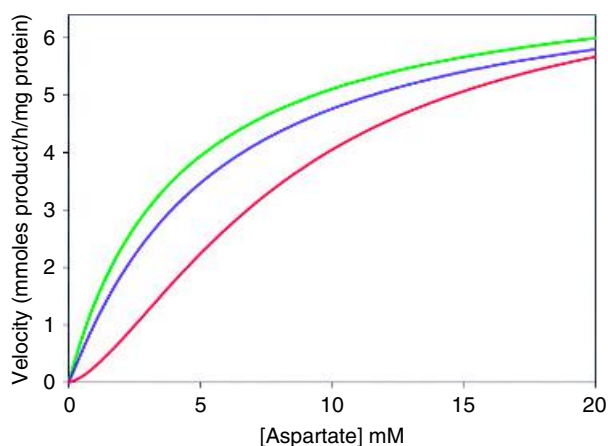


**Figure 7.66** The steady-state kinetic behaviour of ATCase. Carbamoyl aspartate formation at a fixed concentration of substrate (blue) is increased in the presence of ATP (green) whilst CTP has the opposite effect acting as an inhibitor

and to the right in the presence of CTP. At a given substrate concentration CTP diminishes the reaction velocity whilst ATP increases it. ATP is therefore a positive heterotropic effector, CTP a negative heterotropic effector, and aspartate is a positive homotropic effector.

The effects of ATP and CTP are not unexpected; CTP is one product of pyrimidine biosynthesis and inhibition of ATCase activity is an example of feedback inhibition where end products modulate biosynthetic reactions to provide effective means of control (Figure 7.67). Consequently, high intracellular levels of CTP decrease pyrimidine biosynthesis whilst high intracellular levels of ATP indicate an imbalance between purine and pyrimidine concentrations and lead to increased rates of pyrimidine biosynthesis.

Structural insight into allosteric regulation of ATCase is provided by crystallographic analysis of the *E. coli* enzyme by William Lipscomb (Figure 7.68). The enzyme has a composition of  $c_6r_6$  where *c* and *r* represent catalytic and regulatory subunits respectively arranged as two sets of catalytic trimers complexed with three sets of regulatory dimers. Each regulatory dimer links together two subunits present in different trimers. For both catalytic and regulatory subunits two domains exist within each polypeptide chain.

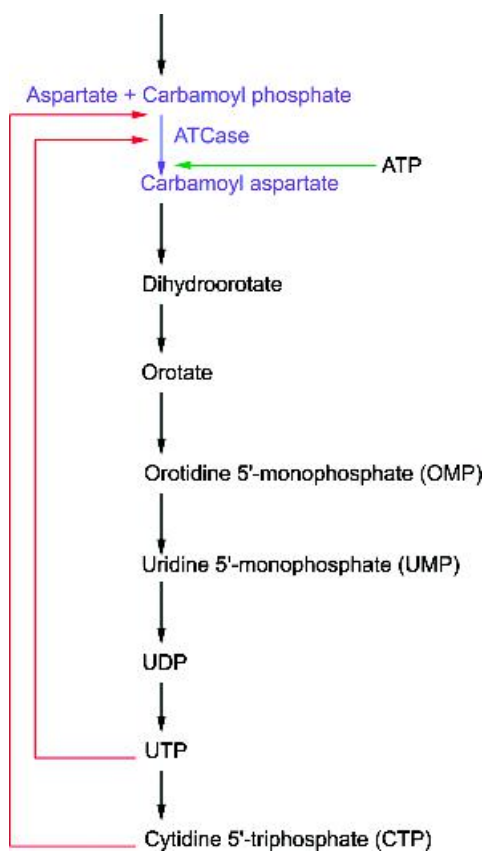


**Figure 7.67** The metabolic pathway leading to UTP and CTP formation – feedback inhibition of ATCase is part of the normal control process

The catalytic subunit (Figure 7.69) contains one domain involved in aspartate binding whilst a second domain binds carbamoyl phosphate with the active site lying between domains. In view of their separation the *c* subunit must undergo large conformational change to bring the sites closer together for product formation. A bifunctional analogue of carbamoyl phosphate and aspartate called *N*-(phosphonacetyl)-*L*-aspartate (PALA) binds to ATCase, but is unreactive and has facilitated structural characterization of the enzyme–substrate complex (Figure 7.70). PALA binds to the R state, and by comparing the structure of this form of the enzyme with that obtained in the T state (ATCase plus CTP) the conformational changes

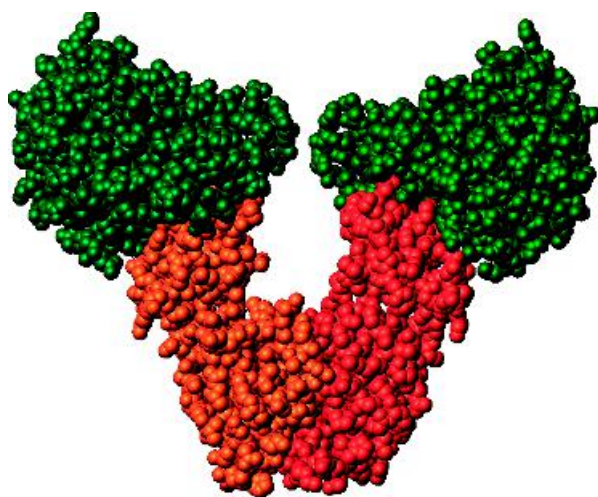


**Figure 7.68** The quaternary structure of ATCase from *E. coli* showing the  $r_2c_6$  structure (PDB: 1ATI). Two regulatory units (orange) link to catalytic subunits (green) belonging to *different* trimers

occurring in transitions from one allosteric form to another were estimated.

The observed kinetic profiles of enzyme activity with ATP and CTP provide further insight into the basis of allosteric regulation. ATP enhances activity and binds to the R state of the enzyme whilst CTP an allosteric inhibitor binds preferentially to the T or low affinity state. Both ATP and CTP bind to the regulatory subunit and compete for the same site. The allosteric binding domain is the larger part of the *r* subunit containing a  $Zn^{2+}$  binding region that forms the interface between the regulatory and catalytic subunits. Displacement of the non-covalently bound Zn using mercurial reagents leads to the absence of binding and the dissociation of the  $c_6r_6$  complex.

The rate of catalysis in isolated trimer is not modulated by ATP or CTP but exceeds the rate observed in the complete enzyme. This kinetic behaviour indicates that *r* subunits reduce the activity of the *c* subunits in the complete enzyme. In view of the different kinetic properties exhibited by ATCase in the presence of ATP or CTP it is somewhat surprising to find that both nucleotides bind in similar manner to the *r* subunit. This makes a structural explanation of

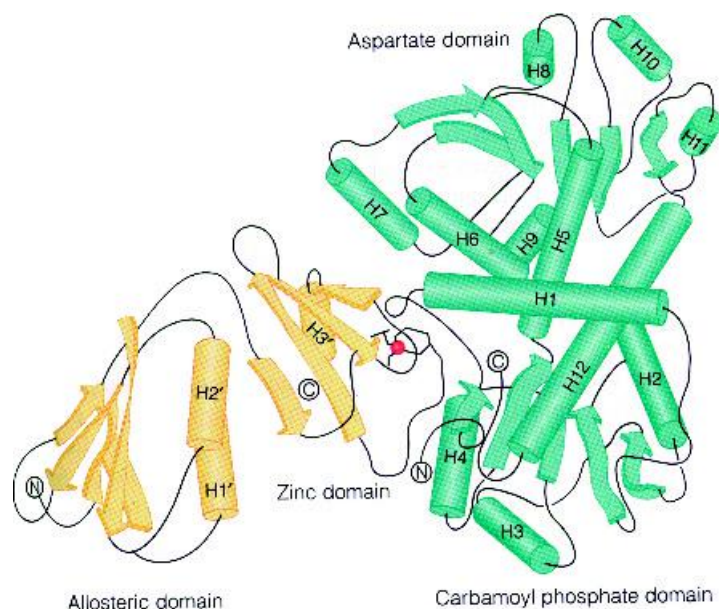


**Figure 7.69** The structure of a single catalytic subunit and its adjacent regulatory subunit. The catalytic subunit is shown in green and the regulatory subunit in yellow (reproduced with permission from Lipscomb, W.N. *Adv. Enzymol.* 1994, **73**, 677–751. John Wiley & Sons)

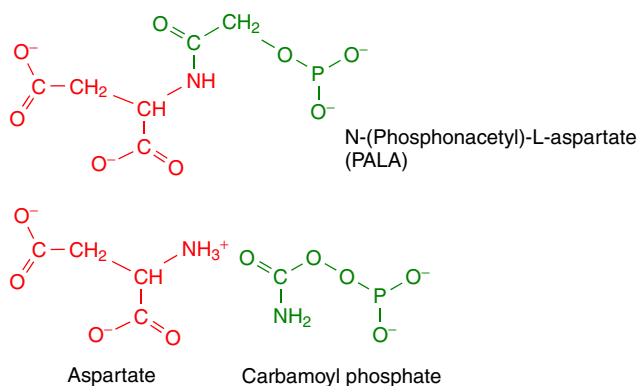


**Figure 7.70** The structure of the bifunctional substrate analogue PALA and its relationship to carbamoyl phosphate and aspartate

their effects difficult to understand and the structural basis of allostery in ATCase has proved very elusive despite structures for the enzyme in the ATCase–CTP complex (T state) and the ATCase–PALA complex (Figure 7.71). A comparison of these two

structures shows that in the T>R transition the enzyme's catalytic trimers separate by  $\sim 1.1$  nm and reorient their axes relative to each other by  $\sim 5^\circ$ . The trimers assume an elongated or eclipse-like configuration along one axis accompanied by rotation of the r



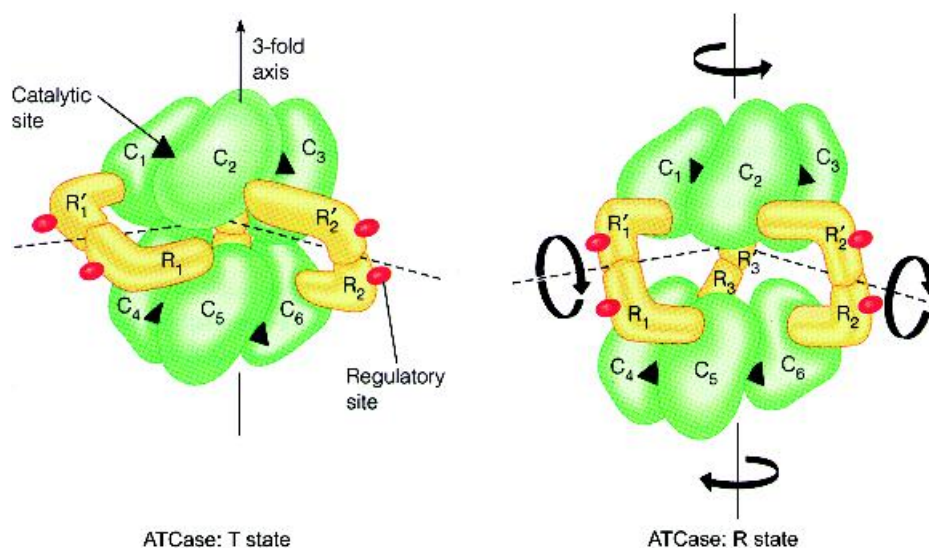


**Figure 7.71** A diagram of the quaternary structure of aspartate transcarbamoylase (ATCase). The quaternary structure in the T state (left) shows six catalytic subunits and six regulatory subunits. Between each catalytic subunit lies the catalytic site whilst on each regulatory subunit is a single effector site on its outer surface (reproduced with permission from Lipscomb, W.N. *Adv. Enzymol.* 1994, **73**, 677–751. John Wiley & Sons)

subunits by  $\sim 15^\circ$  about their two-fold rotational symmetry axis.

## Covalent modification

Covalent modification regulates enzyme activity by the synthesis of *inactive* precursor enzymes containing precursor sequences at the N terminus. Removal of these regions by proteases leads to enzyme activation. Trypsin, chymotrypsin and pepsin are initially synthesized as longer, inactive, precursors called trypsinogen, chymotrypsinogen and pepsinogen or collectively zymogens. Zymogens are common for proteolytic enzymes such as those found in the digestive tracts of mammals where the production of active enzyme could lead to cell degradation immediately after translation. Acute pancreatitis is precipitated by damage to the pancreas resulting from premature activation of digestive enzymes.

Trypsinogen is the zymogen of trypsin and is modified when it enters the duodenum from the pancreas. In the duodenum a second enzyme enteropeptidase secreted from the mucosal membrane excises

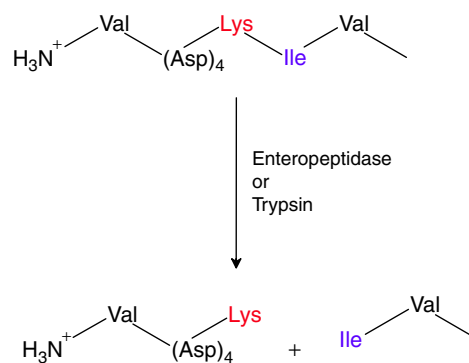


**Figure 7.72** The activation of trypsinogen to trypsin. Limited proteolysis of trypsinogen by enteropeptidase and subsequently trypsin removes a short hexapeptide from the N-terminus

a hexapeptide from the N terminus of trypsinogen to form trypsin (Figure 7.72). Enteropeptidase is itself under hormonal control whilst the site of cleavage after Lys6 is important. The product is trypsin with a natural specificity for cleavage after Lys or Arg residues and

the small amount of trypsin produced is able to catalyse the further production of trypsin from the zymogen. As a result the process is often described as auto-catalytic.

Chymotrypsin is closely related to trypsin and is activated by cleavage of chymotrypsinogen between Lys15 and Val16 to form  $\pi$ -chymotrypsin (Figure 7.73). Further autolysis (self-digestion) to remove residues Ser14-Arg15 and Thr147-Asn148 yields  $\alpha$ -chymotrypsin, the normal form of the enzyme. The three segments of polypeptide chain produced by zymogen processing remain linked by disulfide bridges.

Trypsin plays a major role in the activation of other proteolytic enzymes. Proelastase, a zymogen of elastase, is activated by trypsin by removal of a short N terminal region along with procarboxypeptidases A and B and phospholipase A<sub>2</sub>. The pivotal role of trypsin in zymogen processing requires tight control of trypsinogen activation. At least two mechanisms exist for tight control. Trypsin catalysed activation occurs slowly possibly as a result of the large amount of negative charge in the vicinity of the target lysine residue (four sequential aspartates). This charge repels substrate from the catalytic pocket that also contains

aspartate residues. Zymogens are stored in the pancreas in intracellular vesicles known as zymogen granules that are resistant to proteolytic digestion. As a final measure cells possess serpins that prevent further activation.

A second important group of zymogens are the serine proteases of the blood-clotting cascade (Figure 7.74) that circulate as inactive forms until a stimulus normally in the form of injury to a blood vessel. This rapidly leads to the formation of a clot that prevents further bleeding via the aggregation of platelets within an insoluble network of fibrin. Fibrin is produced from fibrinogen, a soluble blood protein, through the action of thrombin, a serine protease. Thrombin is the last of a long series of enzymes involved in the coagulation process that are sequentially activated by proteolysis of their zymogens. Sequential enzyme activation leads to a coagulation cascade and the overall process allows rapid generation of large quantities of active enzymes in response to biological stimuli.

The concept of programmed cell death or apoptosis is vital to normal development of organisms. For example, the growing human embryo has fingers that are joined by web-like segments of skin. The removal

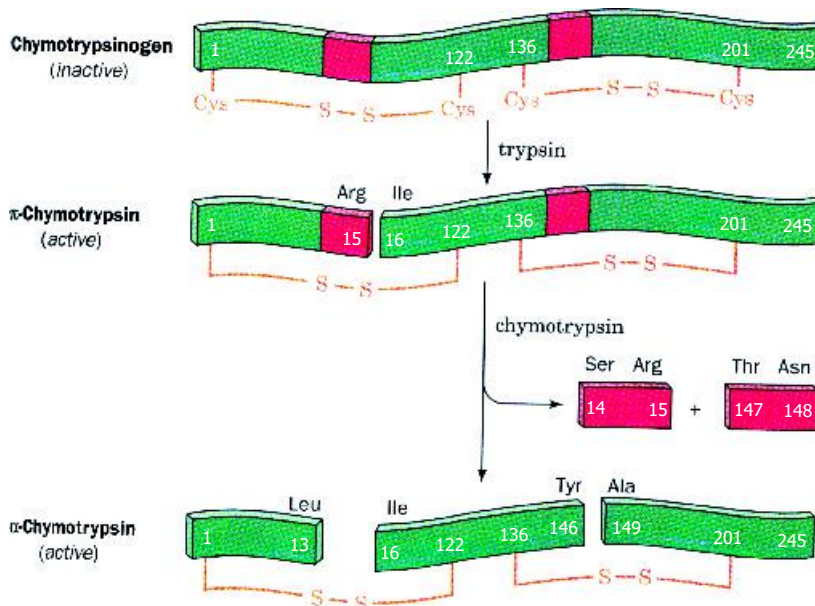


**Figure 7.73** Activation of chymotrypsinogen proceeds through proteolytic processing and the removal of short peptide sequences.

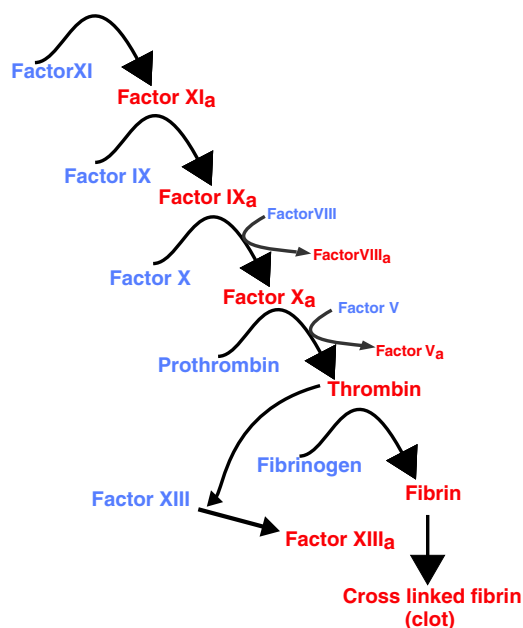


**Figure 7.74** The cascade of enzyme activation during the intrinsic pathway of blood clotting involves processing of serine proteases

of these skin folds and the generation of correct pattern formation (i.e. fingers) relies on a family of intracellular enzymes called caspases. The term caspase refers to the action of these proteins as cysteine-dependent asparsate-specific proteases. Their enzymatic properties are governed by specificity for substrates containing Asp and the use of a Cys285 sidechain for catalysing peptide-bond cleavage located within a conserved motif of five residues (QACRG).

The first level of caspase regulation involves the conversion of zymogens to active forms in response

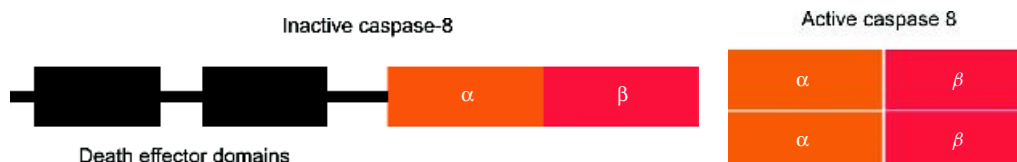
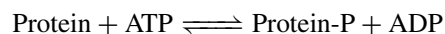


**Figure 7.75** The covalent modification by addition of large protein domains to caspases leads to an inactive enzyme. Their removal allows the association of the  $\alpha$  and  $\beta$  domains in an active heterotetramer

to inflammatory or apoptotic stimuli although second levels of regulation involve specific inhibition of active caspases by natural protein inhibitors. Caspases are synthesized as inactive precursors and their activity is fully inhibited by covalent modification (Figure 7.75). It is important to achieve complete inhibition of activity since the cell is easily destroyed by caspase activity. Caspases are synthesized joined to additional domains known as death effector domains because their removal initiates the start of apoptosis where a significant step is the formation of further active caspases.

Yet another form of enzyme modification is the reversible phosphorylation/dephosphorylation of serine, threonine or tyrosine side chains. The phosphorylation of serine, threonine or tyrosine is particularly important in the area of cell signalling. Phosphorylation of tyrosine is an important covalent modification catalysed by enzymes called protein tyrosine kinases (PTKs). These enzymes transfer the  $\gamma$  phosphate of ATP to specific tyrosine residues on protein substrates according to the reaction



This reaction modulates enzyme activity and leads to the creation of new binding sites for downstream signalling proteins. At least two classes of PTKs are present in cells: the transmembrane receptor PTKs and enzymes that are non-receptor PTKs.

Receptor PTKs are transmembrane glycoproteins activated by ligand binding to an extracellular surface. A conformational change in the receptor results in phosphorylation of specific tyrosine residues on the intracellular domains of the receptor (Figure 7.76) – a process known as autophosphorylation – and initiates activation of many signalling pathways controlling cell proliferation, differentiation, migration

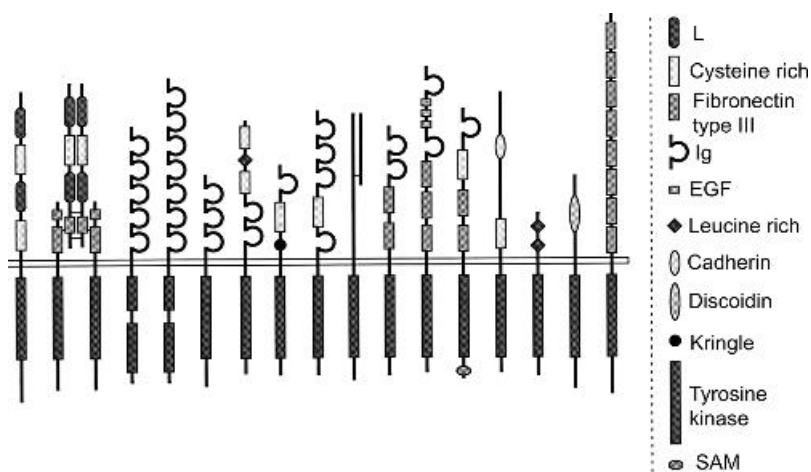


**Figure 7.76** Domain organization of receptor tyrosine kinases. The extracellular domain at the top contains a variety of globular domains arranged with modular architecture. In contrast the cytoplasmic segment is almost exclusively a tyrosine kinase domain (reproduced with permission from Hubbard, S.R. & Till, J.R. *Ann. Rev. Biochem.* 2000, **69**, 373–398. Annual Reviews Inc)

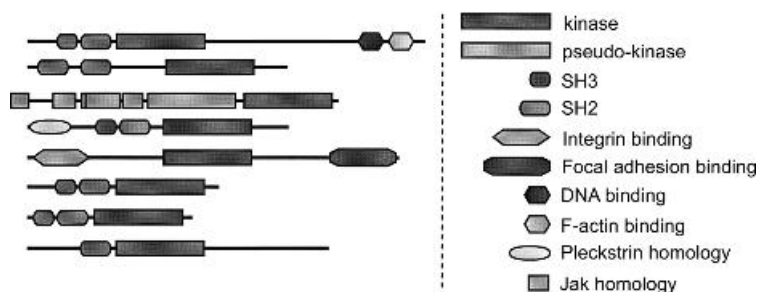


**Figure 7.77** Domain organization found within non-receptor protein kinases (reproduced with permission from Hubbard, S.R. & Till, J.R. *Ann. Rev. Biochem.* 2000, **69**, 373–398. Annual Reviews Inc)

and metabolism. The transmembrane receptor tyrosine kinase family includes the receptors for insulin and many growth factors such as epidermal growth factor, fibroblast growth factor and nerve growth factor. Receptors consist of large extracellular regions constructed from modules of globular domains linked together. A single transmembrane helix links to a cytoplasmic domain possessing tyrosine kinase activity.

In contrast non-receptor PTKs (Figure 7.77) are a large family of proteins that are integral components

of the signal cascades stimulated by RTKs as well as G-protein coupled receptors. These kinases phosphorylate protein substrates causing a switch between active and inactive states. These tyrosine kinases lack large extracellular ligand-binding regions together with transmembrane regions and most are located in the cytoplasm although some bear N-terminal modifications such as myristoylation or palmitoylation that lead to membrane association. In addition to kinase activity this large group of proteins



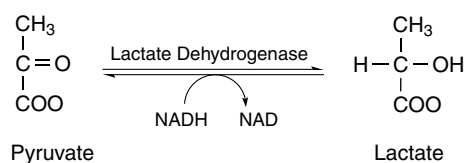


**Figure 7.78** Conversion of pyruvate to lactate by lactate dehydrogenase

Located in the endoplasmic reticulum of cells these enzymes are responsible for the detoxification of drugs and xenobiotics as well as the transformation of substrates such as steroids and prostaglandins. They are described as isoenzymes but arise from different genes containing different primary sequences with active site homology.

An excellent example of an isoenzyme in the second group is lactate dehydrogenase. In the absence of oxygen the final reaction of glycolysis is the conversion of pyruvate to lactic acid catalysed by the enzyme lactate dehydrogenase (LDH) with the conversion of NADH to NAD (Figure 7.78).

In skeletal muscle, where oxygen deprivation is common during vigorous exercise, the reaction is efficient and large amounts of lactate are generated. Under aerobic conditions the reaction catalysed by lactate dehydrogenase is not efficient and pyruvate is preferentially converted to acetyl-CoA. The subunit composition of lactate dehydrogenase is not uniform but varies in different tissues of the body. Five major LDH isoenzymes are found in different vertebrate tissues and each molecule is composed of four polypeptide chains or subunits. LDH is a tetramer and it has been shown that three different primary sequences are detected in human tissues. The three types of LDH chains are M (LDH-A) found predominantly in muscle tissues, H (LDH-B) found in heart muscle together with a more limited form called LDH-C present in the testes of mammals. LDH-C is clearly of restricted distribution within the body and is not considered further. The M and H subunits of LDH are encoded by different genes and as a result of differential gene expression in tissues the tetramer is formed by several different combinations of subunits. Significantly, isoenzymes

of LDH were originally demonstrated by their different electrophoretic mobilities under non-denaturing conditions. Five different forms of LDH were detected; LDH-1, LDH-2, LDH-3, LDH-4, and LDH-5 with LDH-1 showing the lowest mobility. The reasons for these differences in mobility are clear when one compares the primary sequences of the M and H subunits (Figure 7.79).

The H subunit contains a greater number of acidic residues (Asp, Glu) than the M polypeptide. In heart muscle the gene for the H subunit is more active than the gene for the M subunit leading to an LDH enzyme containing more H subunit. Thus, LDH isoenzyme 1 is the predominant form of the enzyme in cardiac muscle. The reverse situation occurs in skeletal muscle where there is more M than H polypeptide produced and LDH-5 is the major form of the enzyme. More importantly, the conversion of pyruvate to lactate increases with the number of M chains and LDH 5 in skeletal muscle contains 4 M subunits and is ideally suited to the conversion of pyruvate to lactate. In contrast LDH-1 has 4 H subunits and is less effective at converting pyruvate into lactate. Lactate dehydrogenase, like many other enzymes, is also found in serum where it is the result of normal cell death. Dying or dead cells liberate cellular enzymes into the bloodstream. The liberation of enzymes into the circulatory system is accelerated during tissue injury and the measurement of LDH isoenzymes in serum has been used to determine the site and nature of tissue injury in humans. For example, when the blood supply to the heart muscle is severely reduced, as occurs in a heart attack, muscle cells die and liberate the enzyme LDH-1 into the bloodstream. An increase in LDH-1 in serum is indicative of a heart attack and may be used diagnostically. In contrast, muscular dystrophy is accompanied by an increase in the levels of LDH-5 derived from dying skeletal muscle cells.

## Summary

Enzymes, with the exception of ribozymes, are catalytic proteins that accelerate reactions by factors up to  $10^{17}$  when compared with the corresponding rate in the uncatalysed reaction. All enzymes can be

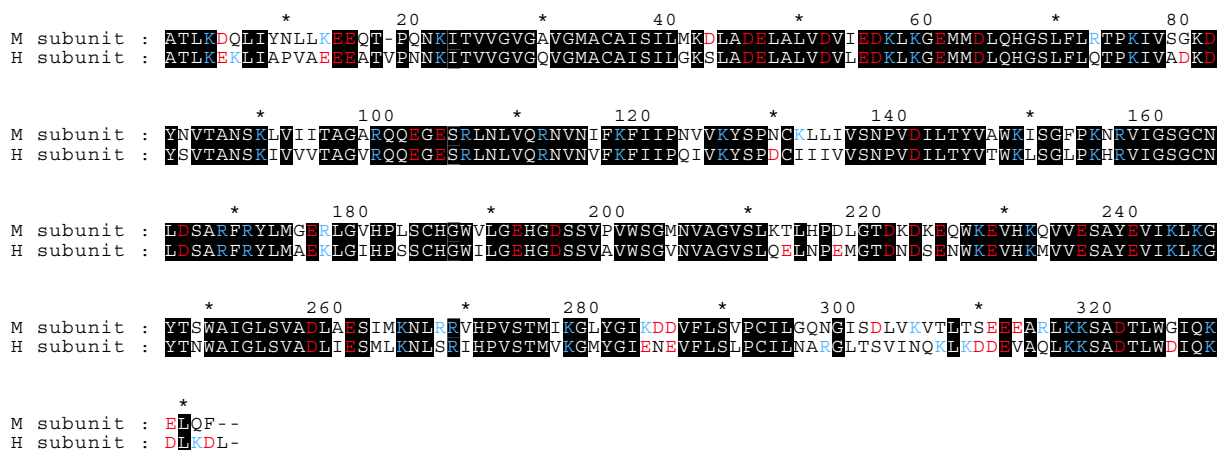


**Figure 7.79** The primary sequences of the M and H subunits of lactate dehydrogenase showing sequence identity (blocks) and the distribution of positively charged side chains (red) and negatively charged side chains (blue) in each sequence. Careful summation of the charged residues reveals that the H subunit has more acidic residues

grouped into one of six functional classes each representing the generic catalytic reaction. These classes are oxidoreductases, transferases, hydrolases, lyases, isomerase and lyases.

Many enzymes require co-factors to perform effective catalysis. These co-factors can be tightly bound to the enzyme including covalent linkage or more loosely associated with the enzyme. Co-factors include metal ions as well as organic components such as pyridoxal phosphate or nicotinamide adenine dinucleotide (NAD). Many co-factors or co-enzymes are derived from vitamins.

All elementary chemical reactions can be described by a rate equation that describes the progress (utilization of initial starting material or formation of product) with time. Reactions are generally described by first or second order rate equations.

Enzymes bind substrate forming an enzyme–substrate complex which then decomposes to yield product. A plot of the velocity of an enzyme-catalysed reaction as a function of substrate concentration exhibits a hyperbolic profile rising steeply at low substrate concentrations before reaching a plateau above which further increases in substrate have little effect on overall rates.

The kinetics of enzyme activity are usually described via the Michaelis–Menten equation that relates the initial velocity to the substrate concentration. This analysis yields several important parameters such as  $V_{\max}$  the maximal velocity that occurs when all the enzyme is found as ES complex,  $K_m$  the substrate concentration at which the reaction velocity is half maximal and  $k_{\text{cat}}/K_m$ , a second order rate constant that represents the catalytic efficiency of enzymes.

Enzymes catalyse reactions by decreasing the activation free energy ( $\Delta G^\ddagger$ ), the energy associated with the transition state. Enzymes use a wide range of catalytic mechanisms to convert substrate into product. These mechanisms include acid–base catalysis, covalent catalysis and metal ion catalysis. Within active sites the arrangement of functional groups allows not only the above catalytic mechanisms but further enhancements via proximity and orientation effects together with preferential binding of the transition state complex. The latter effect is responsible for the greatest enhancement of catalytic activity in enzymes.

The catalytic mechanisms of numerous enzymes have been determined from the application of a combination of structural, chemical modification and kinetic

analysis. Enzymes such as lysozyme, the serine protease family including trypsin and chymotrypsin, triose phosphate isomerase and tyrosinyl tRNA synthetase are now understood at a molecular level and with this level of understanding comes an appreciation of the catalytic mechanisms employed by proteins. Virtually all enzymes employ a combination of mechanisms to achieve effective (rapid and highly specific) catalysis.

Enzyme inhibition represents a vital mechanism for controlling catalytic function. *In vivo* protein inhibitors bind tightly to enzymes causing a loss of activity and one form of regulation. A common form of enzyme inhibition involves the competition between substrate and inhibitor for an active site. Such inhibition is classically recognized from an increase in  $K_m$  whilst  $V_{max}$  remains unaltered. Other forms of inhibition include uncompetitive inhibition where inhibitor binds to the ES complex and mixed (non-competitive) inhibition where binding to both E and ES occurs. Different modes of inhibition are identified from Lineweaver–Burk or Eadie–Hofstee plots.

Irreversible inhibition involves the inactivation of an enzyme by an inhibitor through covalent modification frequently at the active site. Irreversible inactivation is the basis of many forms of poisoning but is also used beneficially in therapeutic interventions with, for example, the modification of prostaglandin  $H_2$  synthase by aspirin alleviating inflammatory responses.

Allosteric enzymes are widely distributed throughout many different cell types and play important roles as regulatory units within major metabolic pathways. Allosteric enzymes contain at least two subunits and often possess many more.

Changes in quaternary structure arise as a result of ligand (effector) binding causing changes in enzyme activity. The conformational changes frequently involve rotation of subunits relative to one another and may produce large overall movement. Such movements are the basis for the transitions between high (R state) and low (T state) affinity states of the enzyme with conformational changes leading to large differences in substrate binding. The ability to modify enzymes via allosteric effectors allows ‘fine-tuning’ of catalytic activity to match fluctuating or dynamic conditions.

Alternative mechanisms of modifying enzyme activity exist within all cells. Most important are covalent modifications that result in phosphorylation or remove parts of the protein, normally the N-terminal region, that limit functional activity. Covalent modification is used in all cells to secrete proteolytic enzymes as inactive precursors with limited proteolysis revealing the fully active protein. Caspases are one group of enzymes using this mechanism of modification and play a vital role in apoptosis. Apoptosis is the programmed destruction of cell and is vital to normal growth and development. Premature apoptosis is serious and caspases must be inactivated via covalent modification to prevent unwanted cell death.

## Problems

1. Consult an enzyme database and find three examples of each major class of enzyme. (i.e. three from each of the six groupings).
2. Describe the effect of increasing temperature and pH on enzyme-catalysed reactions.
3. How can some enzymes work at pH 2.0 or at 90°C. Illustrate your answer with selective example enzymes.
4. Draw a transition state diagram of energy versus reaction coordinate for uncatalysed and an enzyme catalysed reactions.
5. How is the activity of many dehydrogenases most conveniently measured. How can this method be exploited to measure activity in other enzymes?
6. Identify nucleophiles used by enzymes in catalysis?
7. Why does uncompetitive inhibition lead to a decrease in  $K_m$ ? What happens to the  $V_{max}$ ?
8. An enzyme is found to have an active site cysteine residue that plays a critical role in catalysis. At what pH does this cysteine operate efficiently in nucleophilic catalysis? Describe how proteins alter the  $pK$  of this side chain from its normal value in



- solution. What would you expect the effect to be on the catalysed reaction?
9. Construct a plot of initial velocity against substrate concentration from the following data. Estimate values of  $K_m$  and  $V_{max}$ . Repeat the calculation of  $K_m$  and  $V_{max}$  to yield improved estimates.
10. In a second enzyme kinetic experiment the initial velocity of an enzyme catalysed reaction was followed in the presence of native substrate and at five different concentrations of an inhibitory substrate. The following data were obtained. Interpret the results.

Substrate concentration ( $\mu\text{M}$ )	Initial velocity ( $\mu\text{mol s}^{-1}$ )
25.0	80.0
50.0	133.3
75.0	171.4
100.0	200.0
200.0	266.6
300.0	300.0
400.0	320.0
600.0	342.8
800.0	355.5

Substrate concentration ( $\mu\text{M}$ )	Initial velocity ( $\mu\text{mol s}^{-1}$ )	Inhibitor 50 $\mu\text{M}$	Inhibitor 150 $\mu\text{M}$	Inhibitor 250 $\mu\text{M}$	Inhibitor 350 $\mu\text{M}$	Inhibitor 450 $\mu\text{M}$
20	90.91	62.50	38.46	27.78	21.74	17.86
40	166.67	117.65	74.07	54.05	42.55	35.09
60	230.77	166.67	107.14	78.95	62.50	51.72
80	285.71	210.53	137.93	102.56	81.63	67.80
100	333.33	250.00	166.67	125.00	100.00	83.33
125	384.62	294.12	200.00	151.52	121.95	102.04
150	428.57	333.33	230.77	176.47	142.86	120.00
200	500.00	400.00	285.71	222.22	181.82	153.85
250	555.56	454.55	333.33	263.16	217.39	185.19
300	600.80	500.83	375.78	300.70	250.62	214.85
400	666.67	571.43	444.44	363.64	307.69	266.67
500	714.29	625.00	500.00	416.67	357.14	312.50
600	750.00	666.67	545.45	461.54	400.00	352.94
800	800.00	727.27	615.38	533.33	470.59	421.05
1000	833.33	769.23	666.67	588.24	526.32	476.19

